Results

III. RESULTS

In this chapter the results obtained from different electrochemical studies and weight-loss studies, which had been carried out to evaluate the performance of benzylideneaniline derivatives as inhibitors for the corrosion of copper and its different alloys such as muntz, admiralty brass, and arsenical aluminium brass in 0.5M HCl are presented.

3.1- WEIGHT LOSS MEASUREMENTS

Table (3.1) gives the self-corrosion rates of copper and its alloys in 0.5M HCl. Values of inhibition efficiency for different concentrations of benzylideneaniline derivatives ranging from $1x10^{-6}$ to $11x10^{-6}$M for the corrosion of copper and its different alloys in 0.5M HCl solution are given in tables (3.2 - 3.5.) It can be seen from these tables that all these compounds inhibit the corrosion of copper and its alloys in HCl corrosion media.

The obtained weight loss-time curves for copper and its alloys in 0.5M HCl are shown in Figs. (3.1-3.20) and they are characterized by a sharp rise in weight loss from the beginning. Curves for additives containing system fall below that of the free acid. These curves indicated that, the weight loss of copper and its alloys depends on both the type and concentration of additives. Increase in bulk concentration and consequently increase of surface coverage by the additive increases their inhibition efficiency as indicated by the decrease in weight loss per cm^2.

Table (3.1). Corrosion rates of copper and its alloys in 0.5M HCl.

Sl. No.	Material used	Corrosion rate in mpy
1	Pure copper	66.2
2	Muntz alloy	73.1
3	Admiralty brass	70.4
4	Arsenical aluminium	55

Table (3.2). Values of inhibition efficiencies for different benzylideneaniline derivatives for the corrosion of muntz in 0.5M HCl solution.

Duration of the experiment: 180 mins. Temperature: 30 ± 0.2°C.

Concentration (M)	Inhibition efficiency (I.E %)				
	a	b	c	d	e
$1x10^{-6}$	14	10	13	17	19
$3x10^{-6}$	30	25	28	32	34
$5x10^{-6}$	48	44	46	51	55
$7x10^{-6}$	65	60	63	67	71
$9x10^{-6}$	75	72	74	77	78
$11x10^{-6}$	81	80	81	82	83

Table (3.3). Values of inhibition efficiencies for different benzylideneaniline derivatives for the corrosion of admiralty in 0.5M HCl solution.

Duration of the experiment: 180 mins. Temperature: 30 ± 0.2°C.

Concentration (M)	Inhibition efficiency (I.E %)				
	a	b	c	d	e
$1x10^{-6}$	14	12	13	15	16
$3x10^{-6}$	28	26	27	29	30
$5x10^{-6}$	47	45	46	48	50
$7x10^{-6}$	64	61	62	66	68
$9x10^{-6}$	75	73	74	76	77
$11x10^{-6}$	82	80	81	83	84

Table (3.4). Values of inhibition efficiencies for different benzylideneaniline derivatives for the corrosion of copper in 0.5M HCl solution.

Duration of the experiment: 180 mins. Temperature: 30 ± 0.2°C.

Concentration (M)	Inhibition efficiency (I.E %)				
	a	b	c	d	e
$1x10^{-6}$	13	10	11	14	16
$3x10^{-6}$	28	26	27	30	33
$5x10^{-6}$	49	48	48	53	56
$7x10^{-6}$	69	66	67	71	75
$9x10^{-6}$	78	76	77	79	82
$11x10^{-6}$	86	84	85	87	89

Table (3.5). Values of inhibition efficiencies for different benzylideneaniline derivatives for the corrosion of arsenic in 0.5M HCl solution.

Duration of the experiment: 180 mins. Temperature: 30 ± 0.2°C.

Concentration (M)	Inhibition efficiency (I.E %)				
	a	b	c	d	e
$1x10^{-6}$	14	13	14	15	16
$3x10^{-6}$	29	27	28	30	32
$5x10^{-6}$	48	46	47	49	51
$7x10^{-6}$	64	62	63	67	68
$9x10^{-6}$	76	74	75	77	79
$11x10^{-6}$	81	79	80	82	84

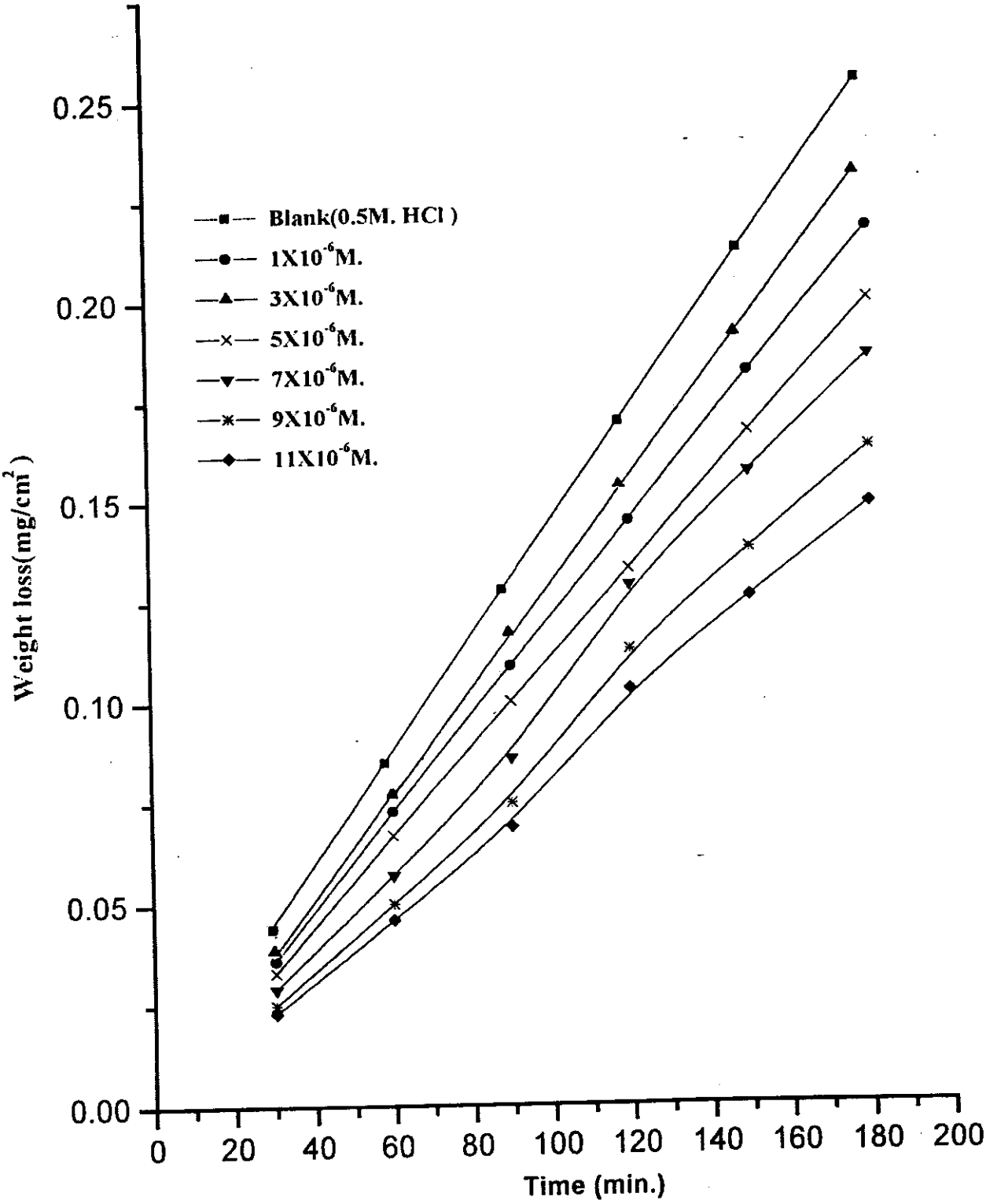

Fig. (3.1) Weight loss - time curves for corrosion of muntz in presence and absence of different concentrations of compound (a) at 30°C.

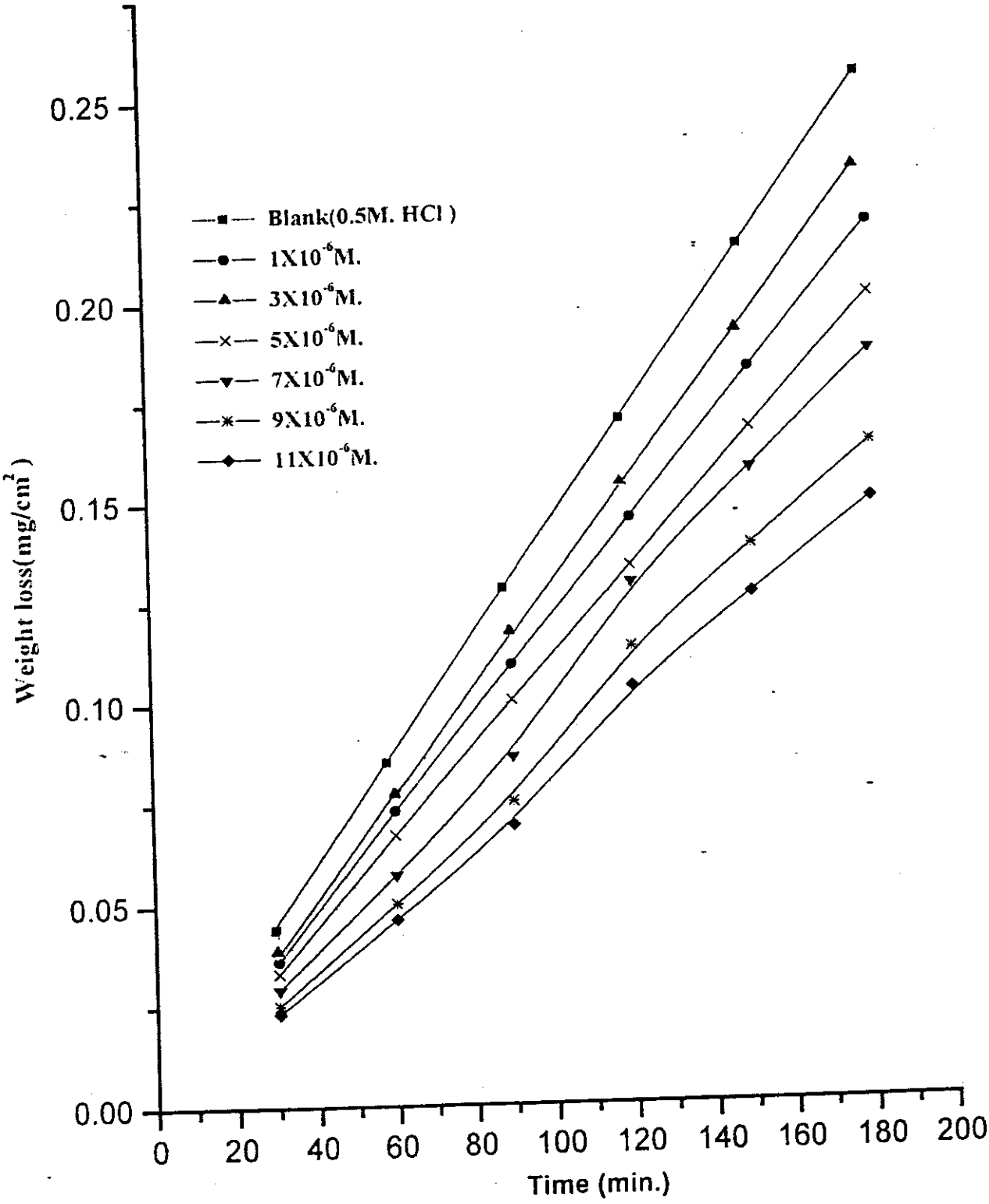

Fig. (3.1) Weight loss - time curves for corrosion of muntz in presence and absence of different concentrations of compound (a) at 30°C.

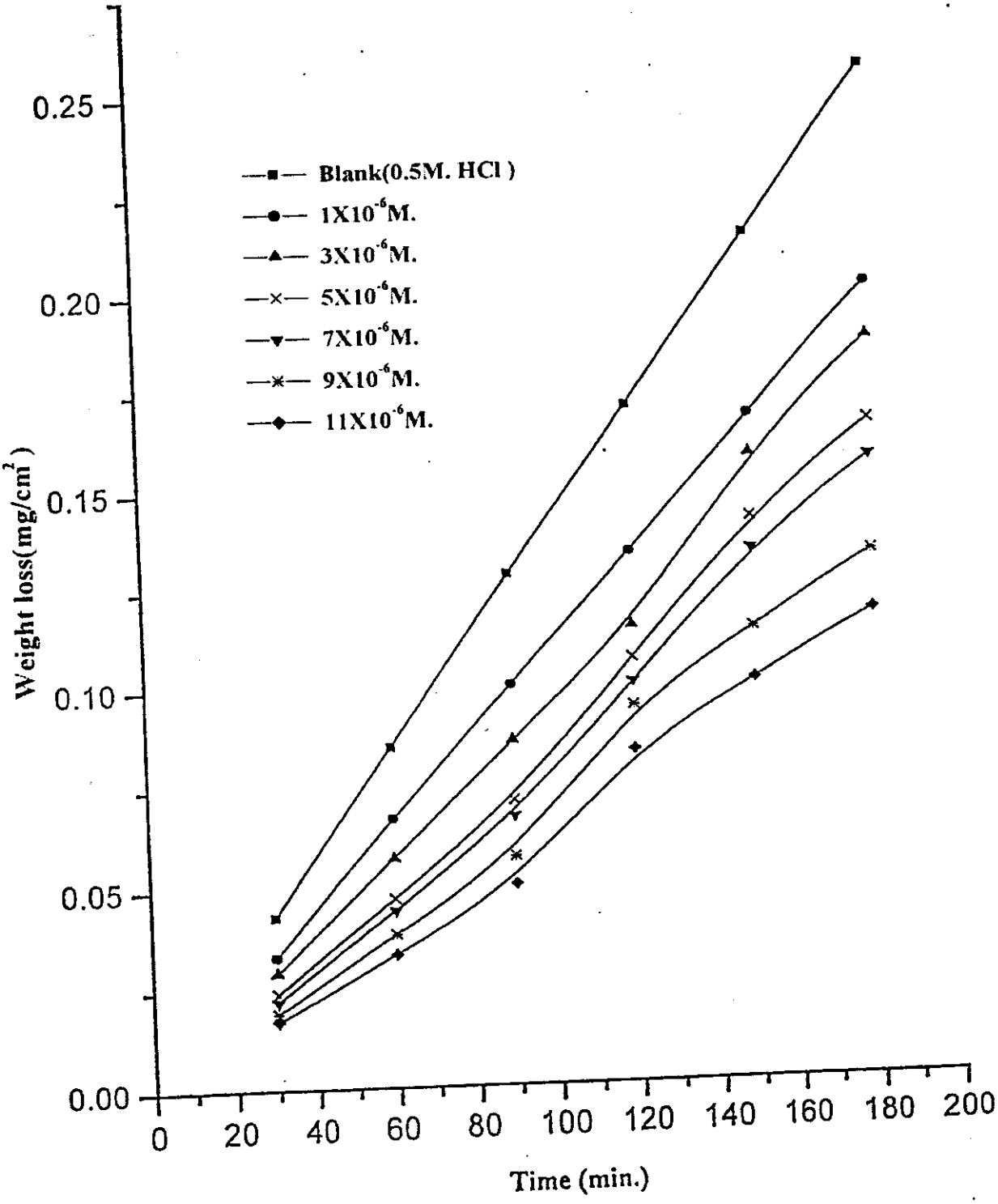

Fig. (3.2) Weight loss - time curves for corrosion of muntz in presence and absence of different concentrations of compound (b) at 30°C.

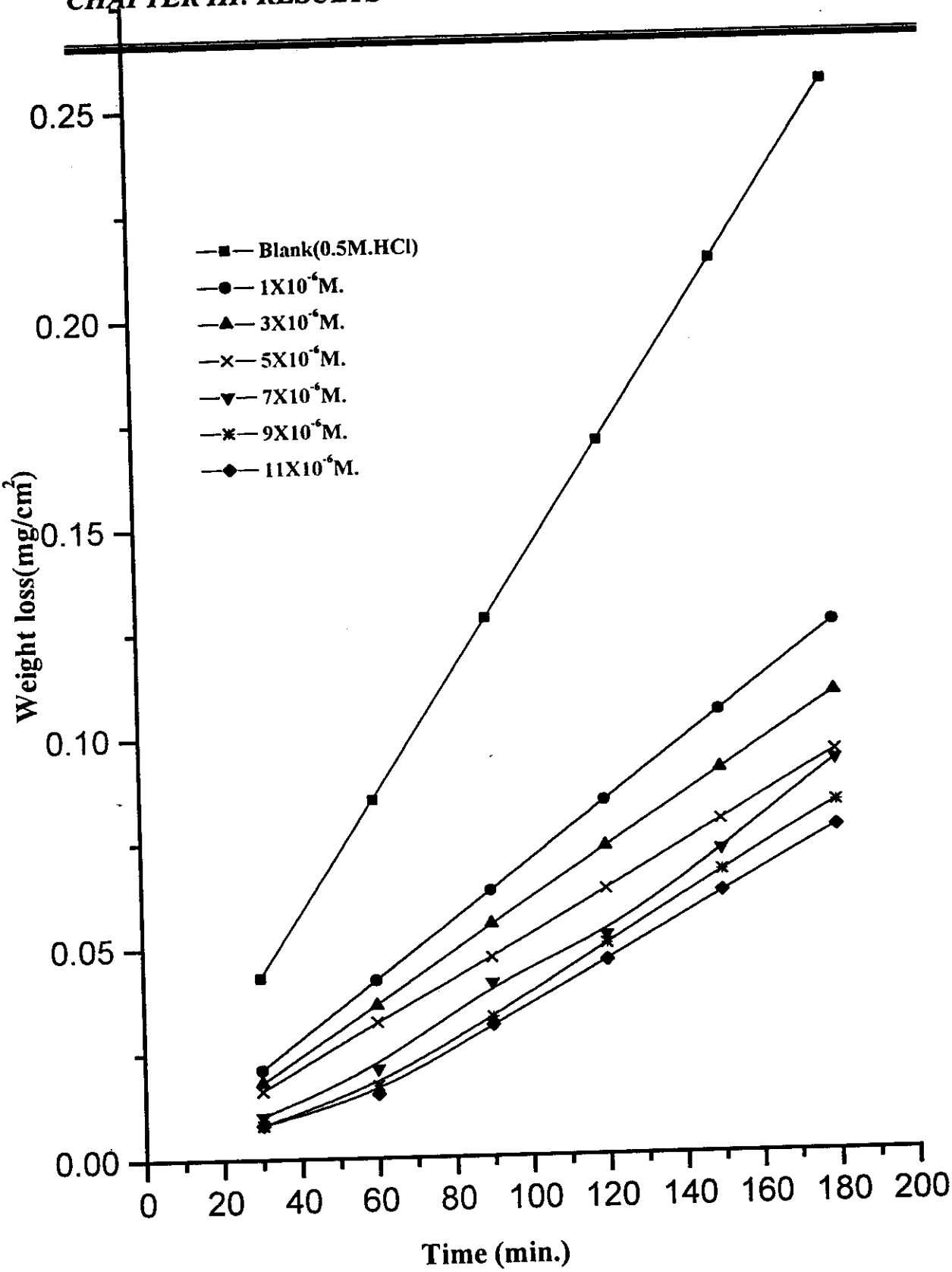

Fig. (3.3) Weight loss - time curves for corrosion of muntz in presence and absence of different concentrations of compound (c) at 30° C.

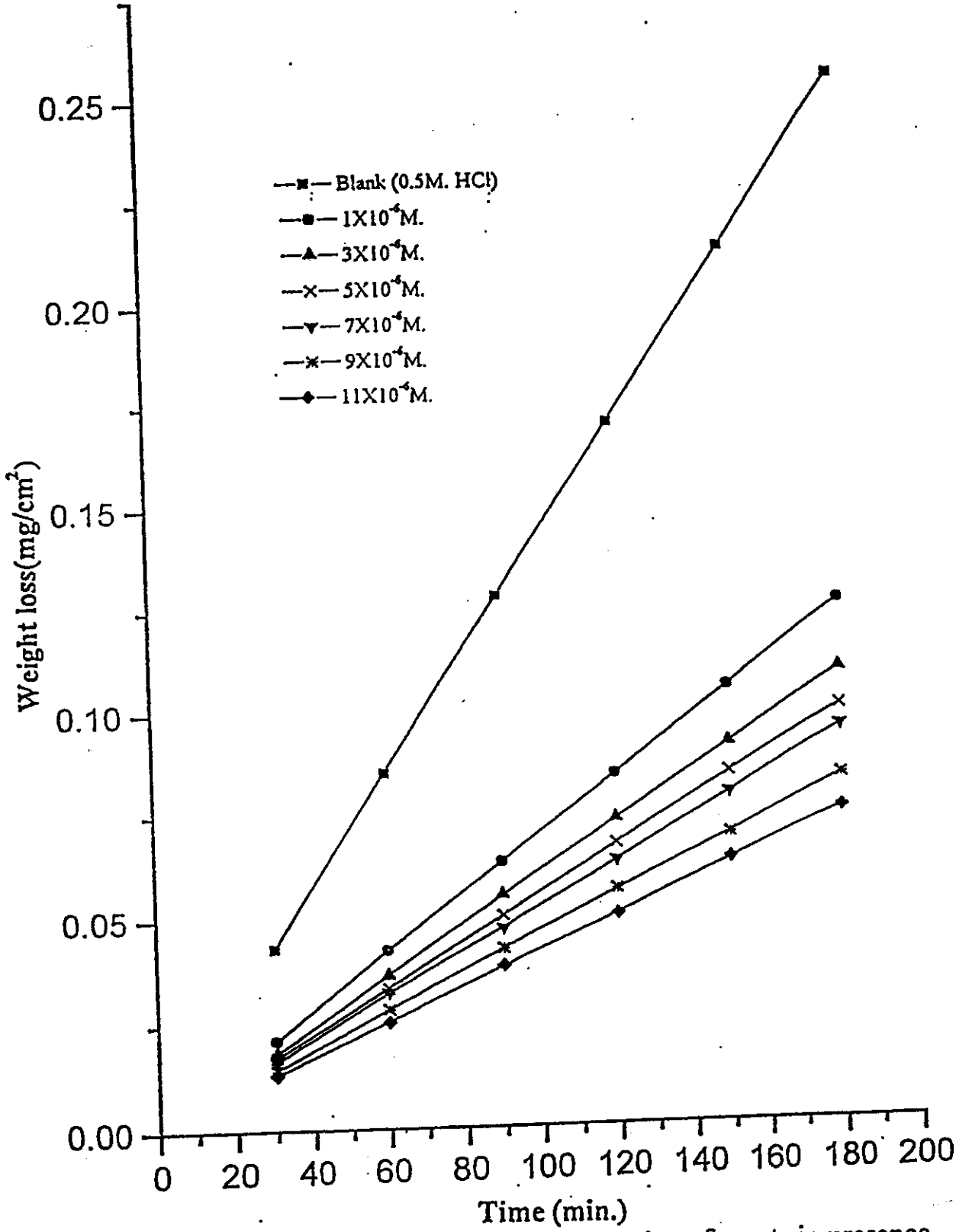

Fig. (3.4) Weight loss - time curves for corrosion of muntz in presence and absence of different concentrations of compound (d) at 30°C

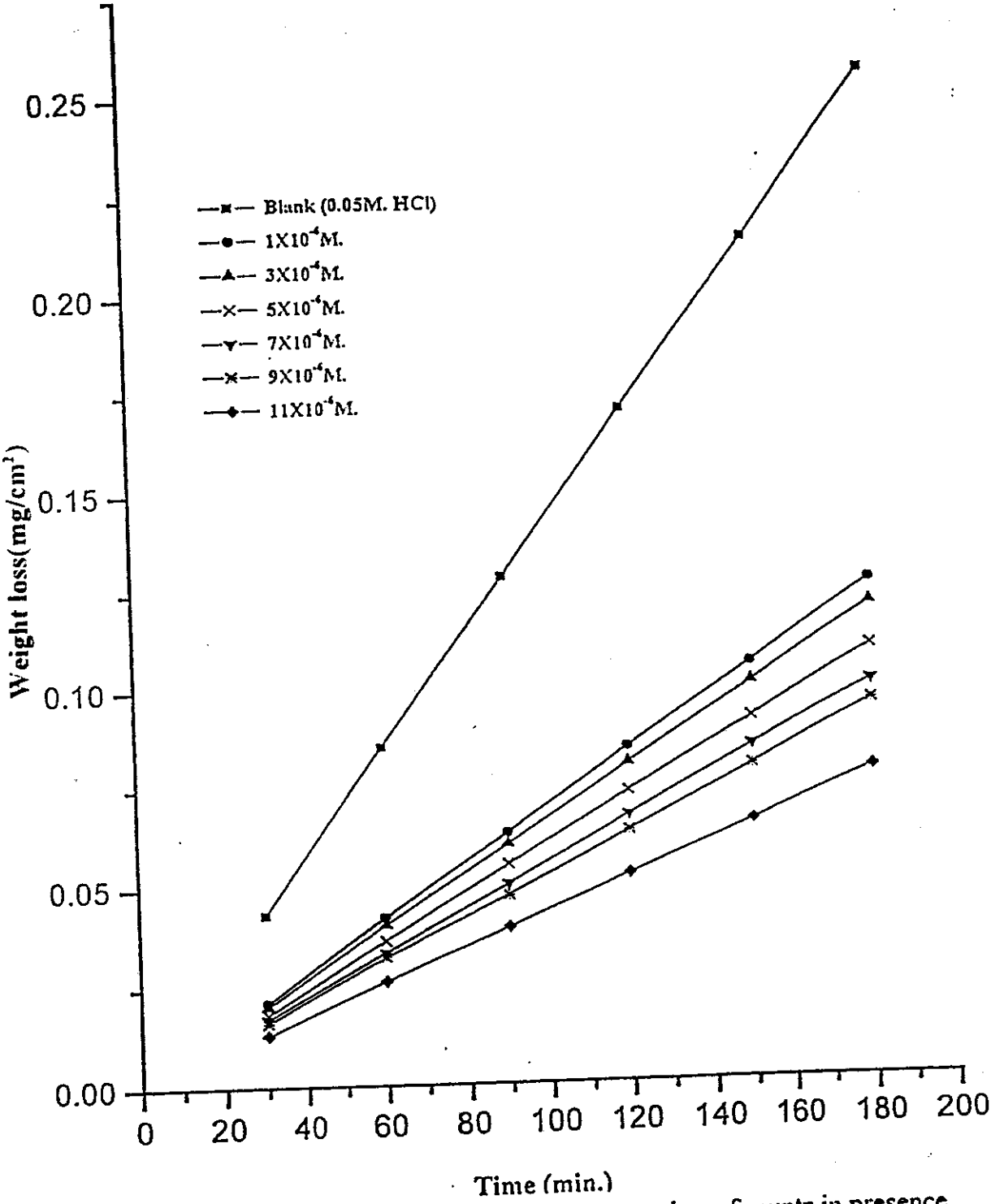

Fig. (3.5) Weight loss - time curves for corrosion of muntz in presence and absence of different concentrations of compound (e) at 30° C.

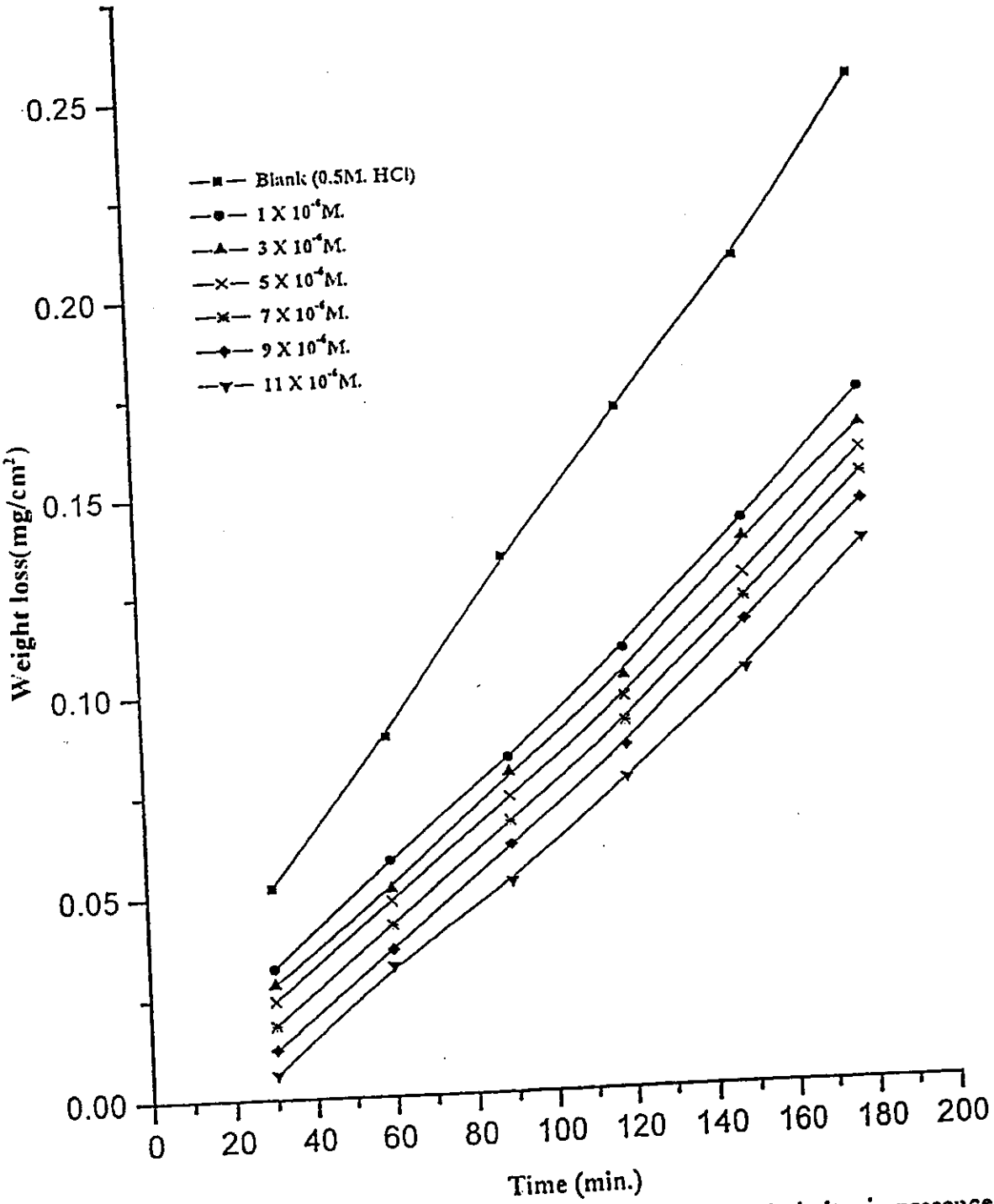

Fig. (3.6) Weight loss - time curves for corrosion of admiralty in presence and absence of different concentrations of compound (a) at 30°C.

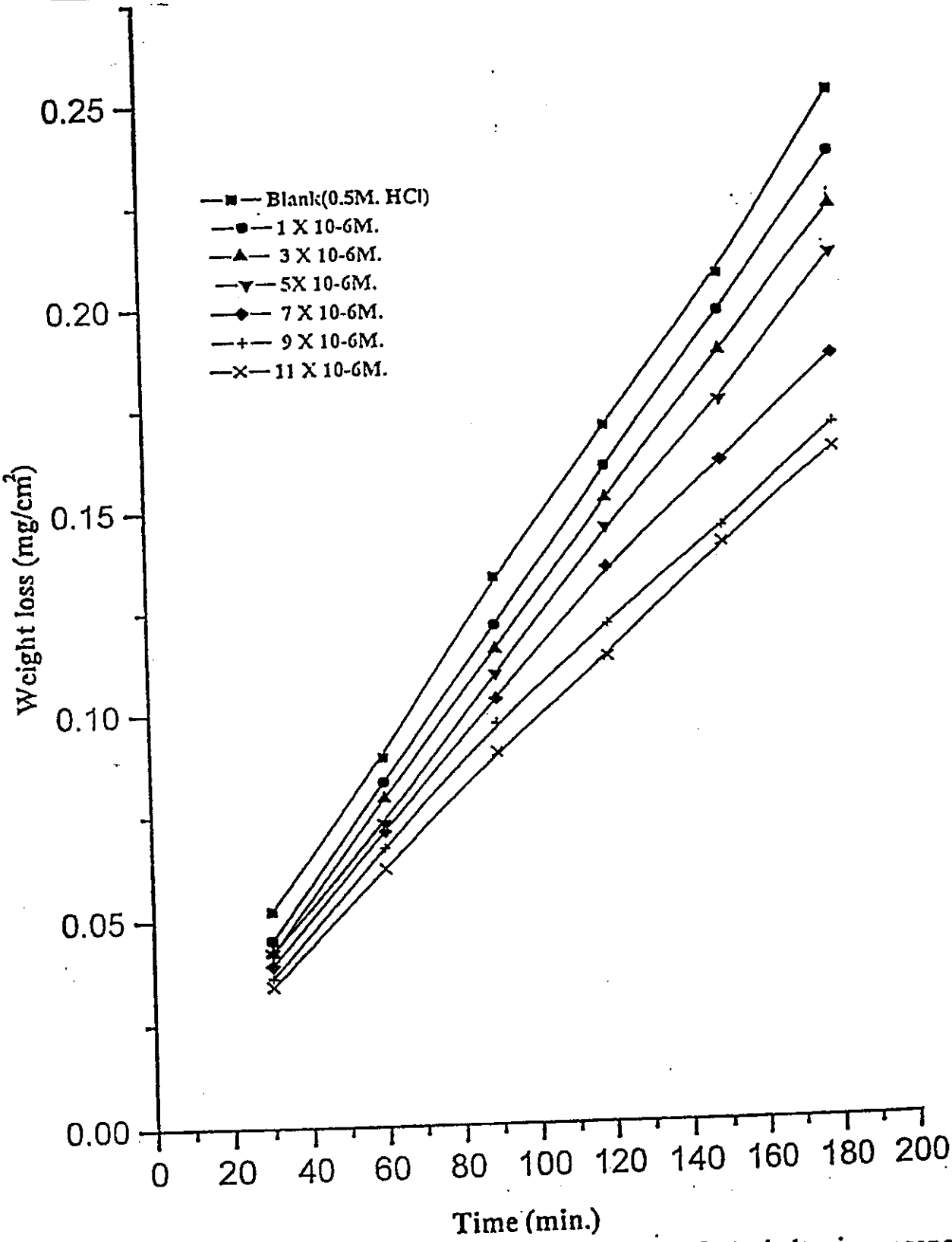

Fig. (3.7) Weight loss - time curves for corrosion of admiralty in presence and absence of different concentrations of compound (b) at 30°C.

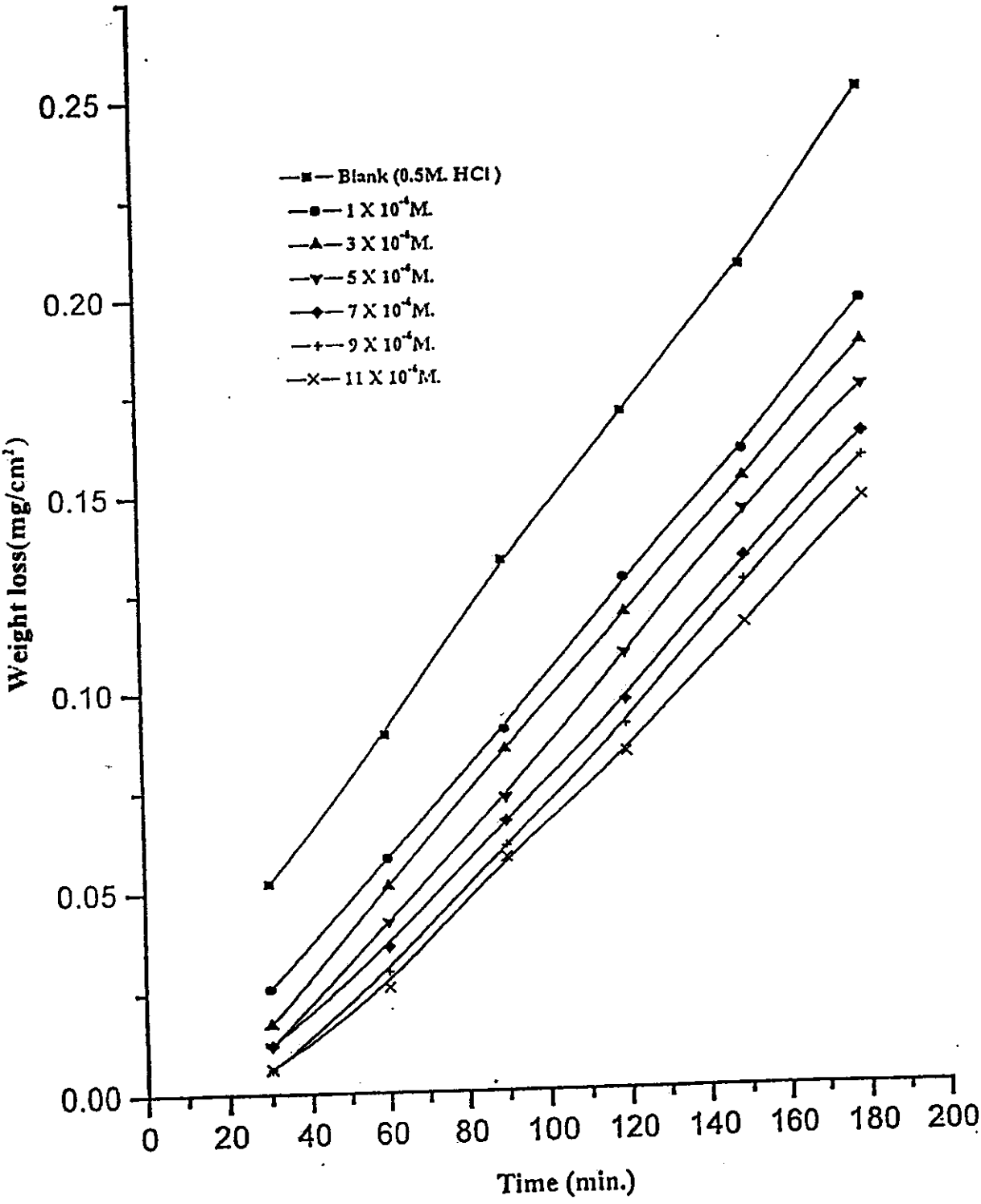

Fig. (3.8) Weight loss - time curves for corrosion of admiralty in presence and absence of different concentrations of compound (c) at 30°C.

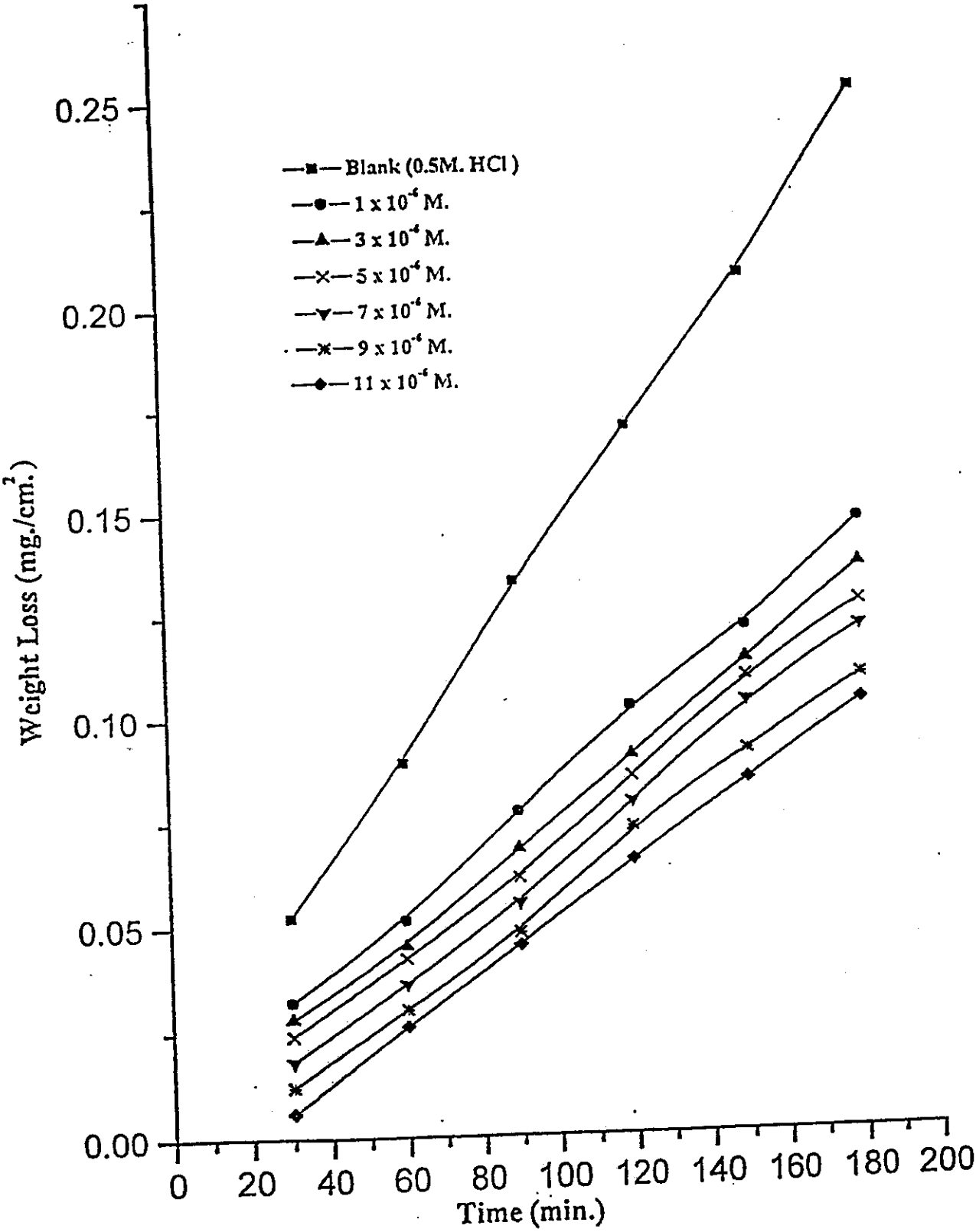

Fig. (3.9) Weight loss - time curves for corrosion of admiralty in presence and absence of different concentrations of compound (d) at30°C.

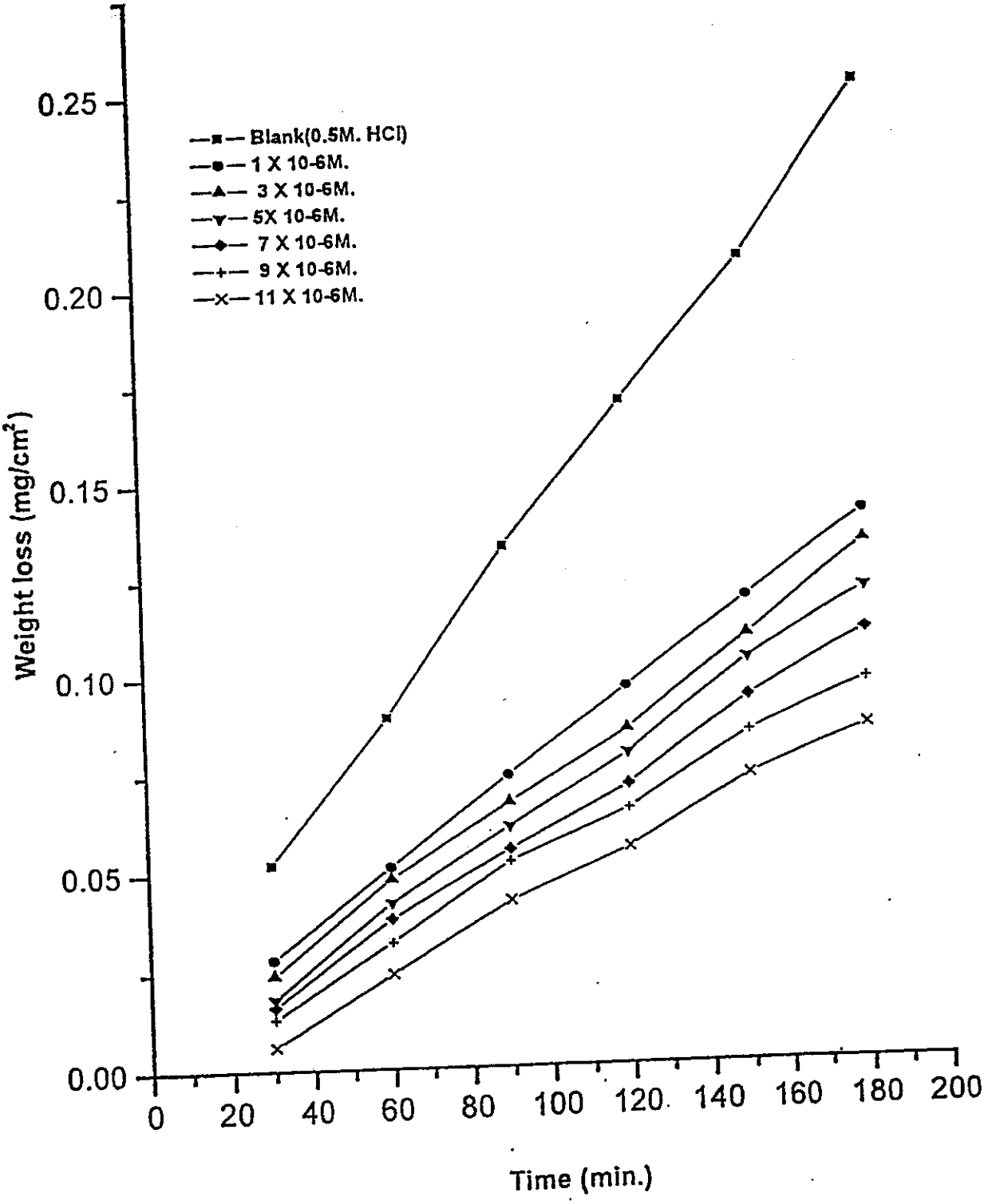

Fig. (3.10) Weight loss - time curves for corrosion of admiralty in presence and absence of different concentrations of compound (e) at 30°C.

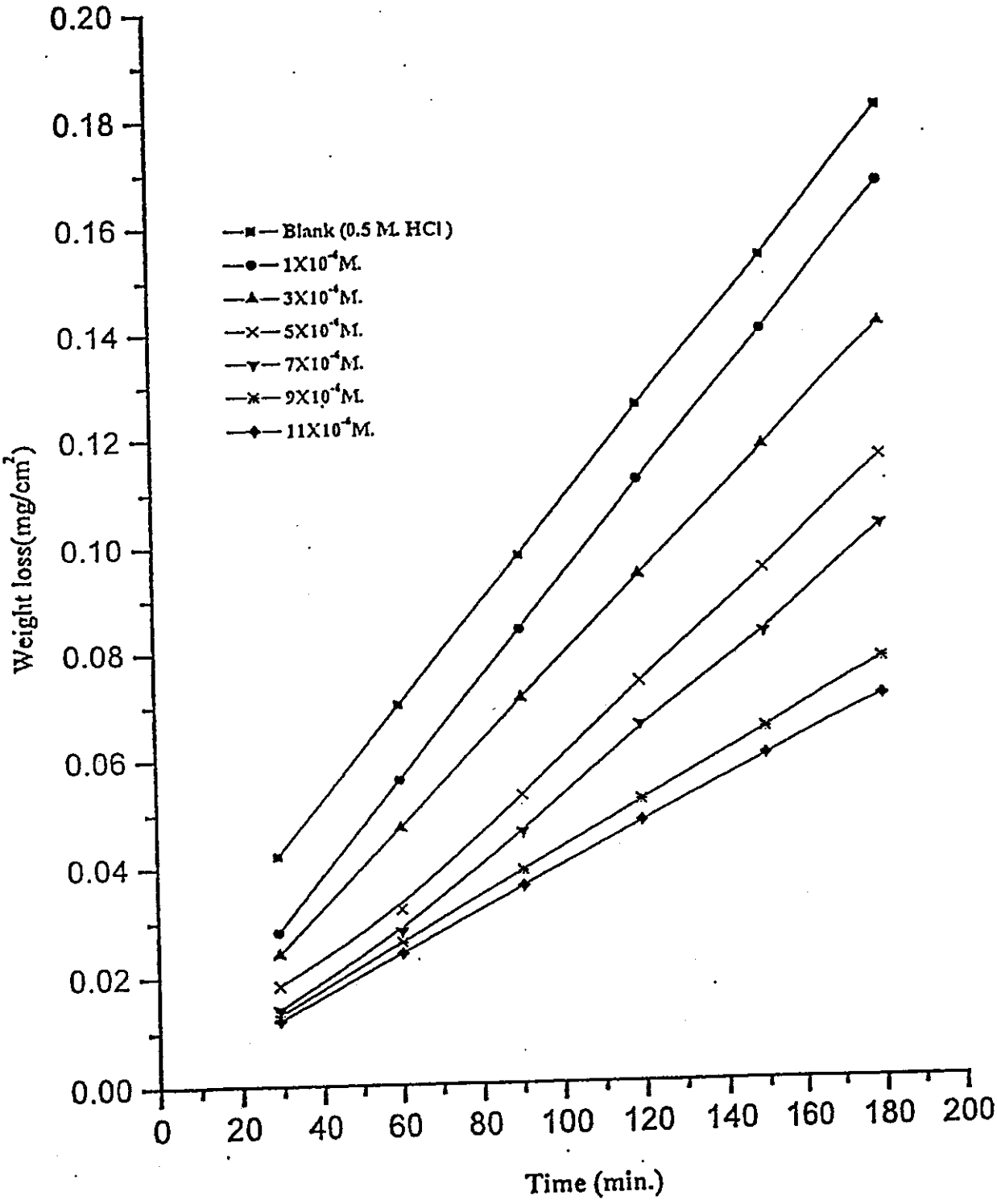

Fig. (3.11) Weight loss - time curves for corrosion of copper in presence and absence of different concentrations of compound (a) at 30° C

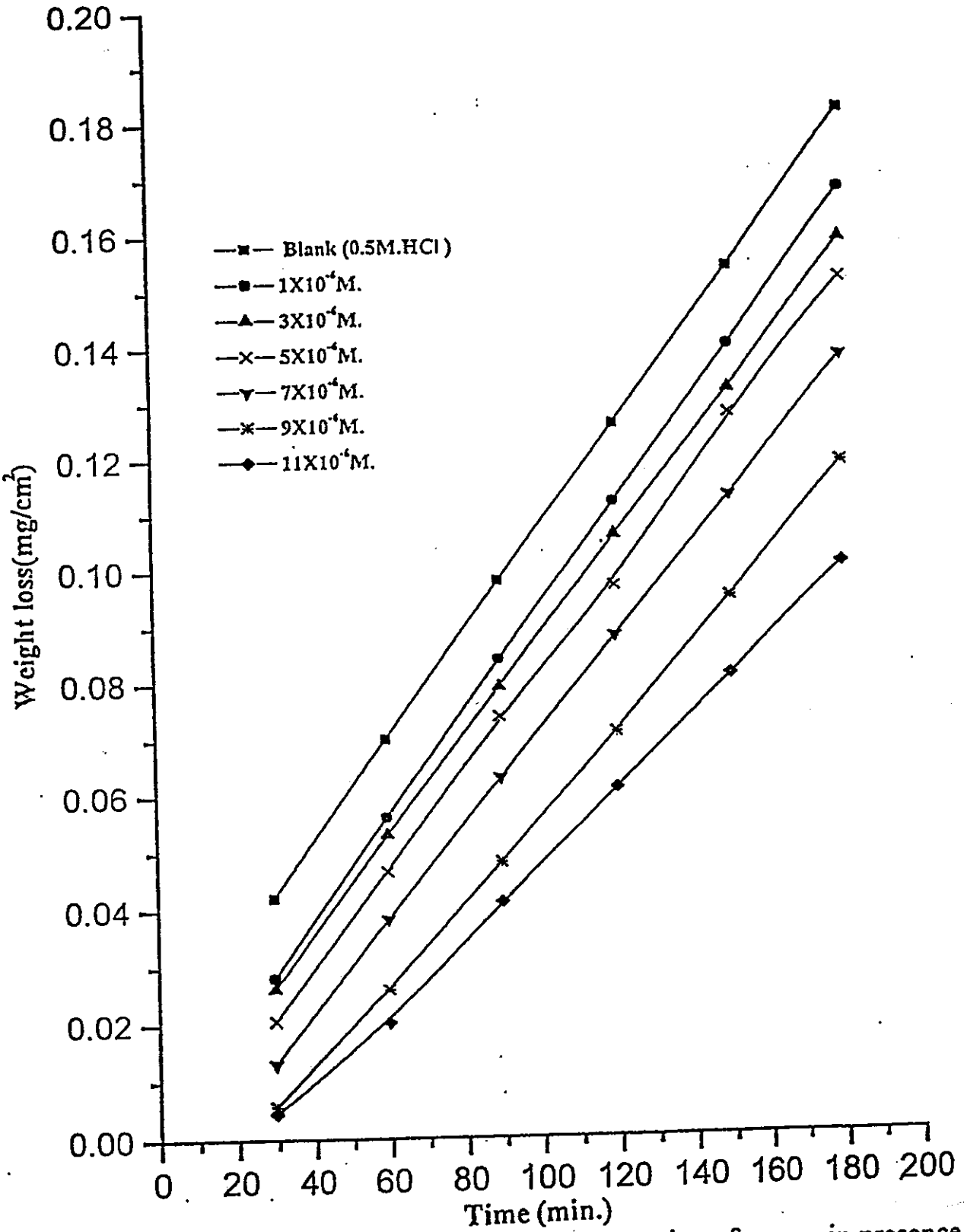

Fig. (3.12) Weight loss - time curves for corrosion of copper in presence and absence of different concentrations of compound (b) at 30° C

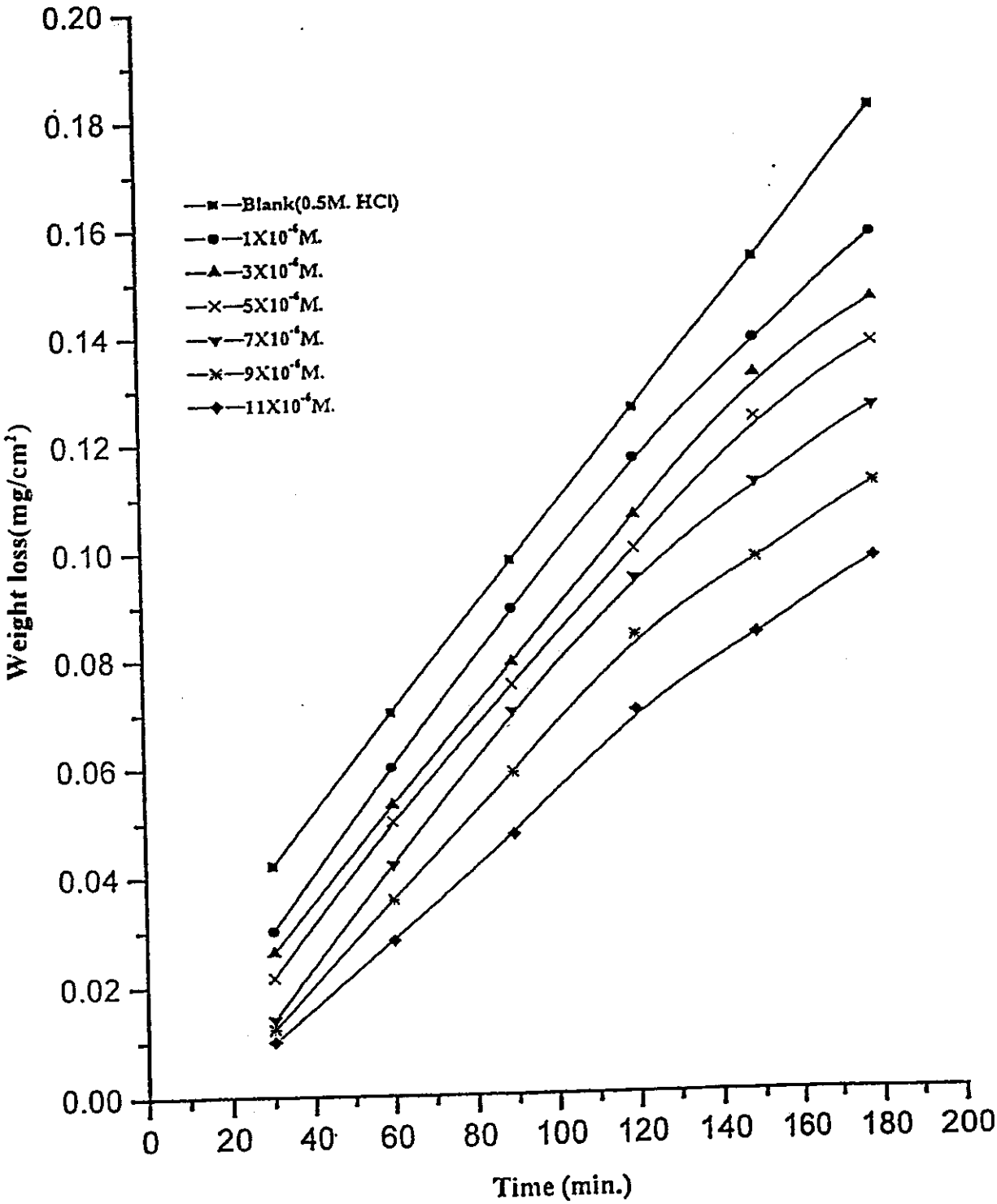

Fig. (3.13) Weight loss - time curves for corrosion of copper in presence and absence of different concentrations of compound (c) at 30°C

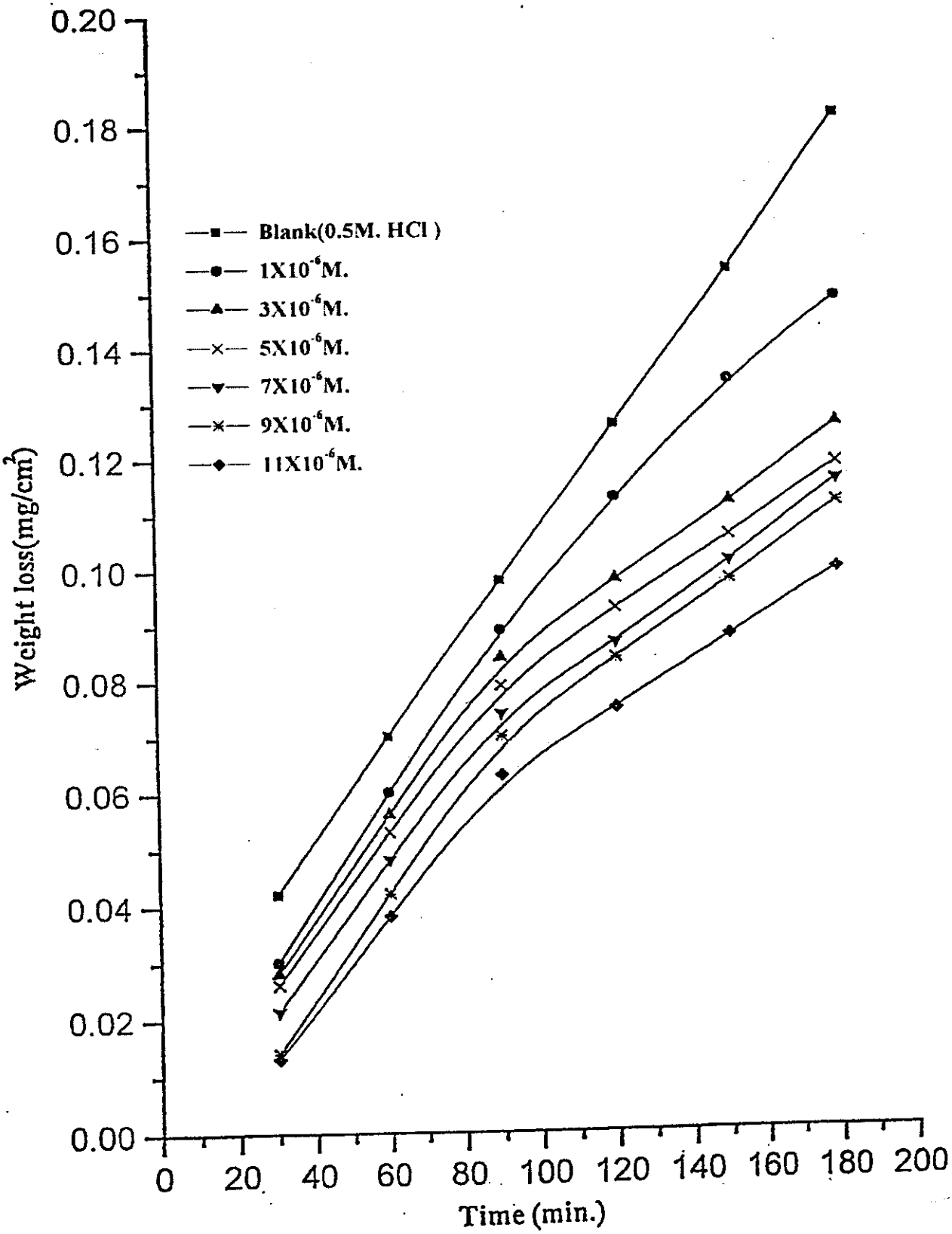

Fig. (3.14) Weight loss - time curves for corrosion of copper in presence and absence of different concentrations of compound (d) at 30°C

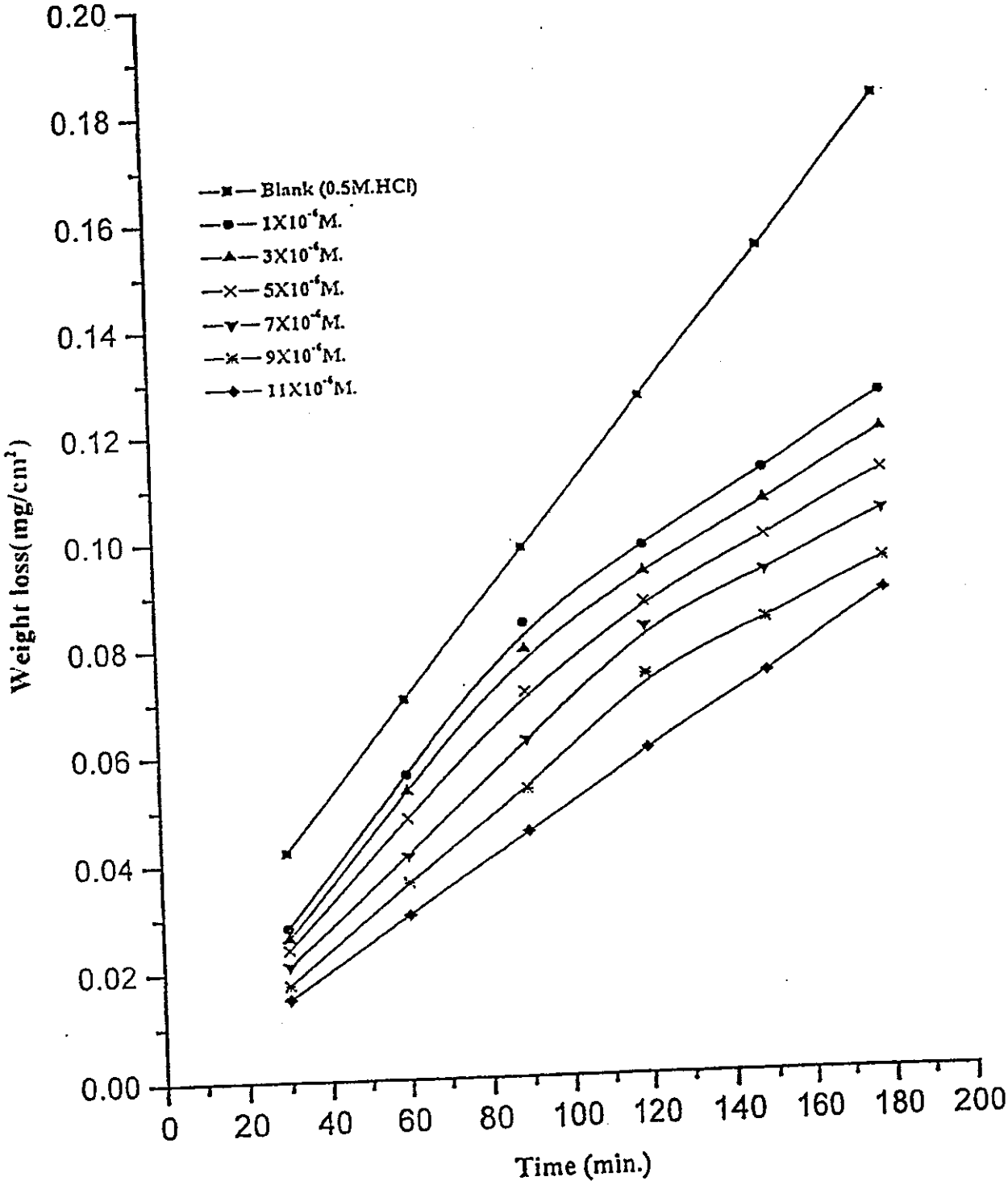

Fig. (3.15) Weight loss - time curves for corrosion of copper in presence and absence of different concentrations of compound (e) at 30° C

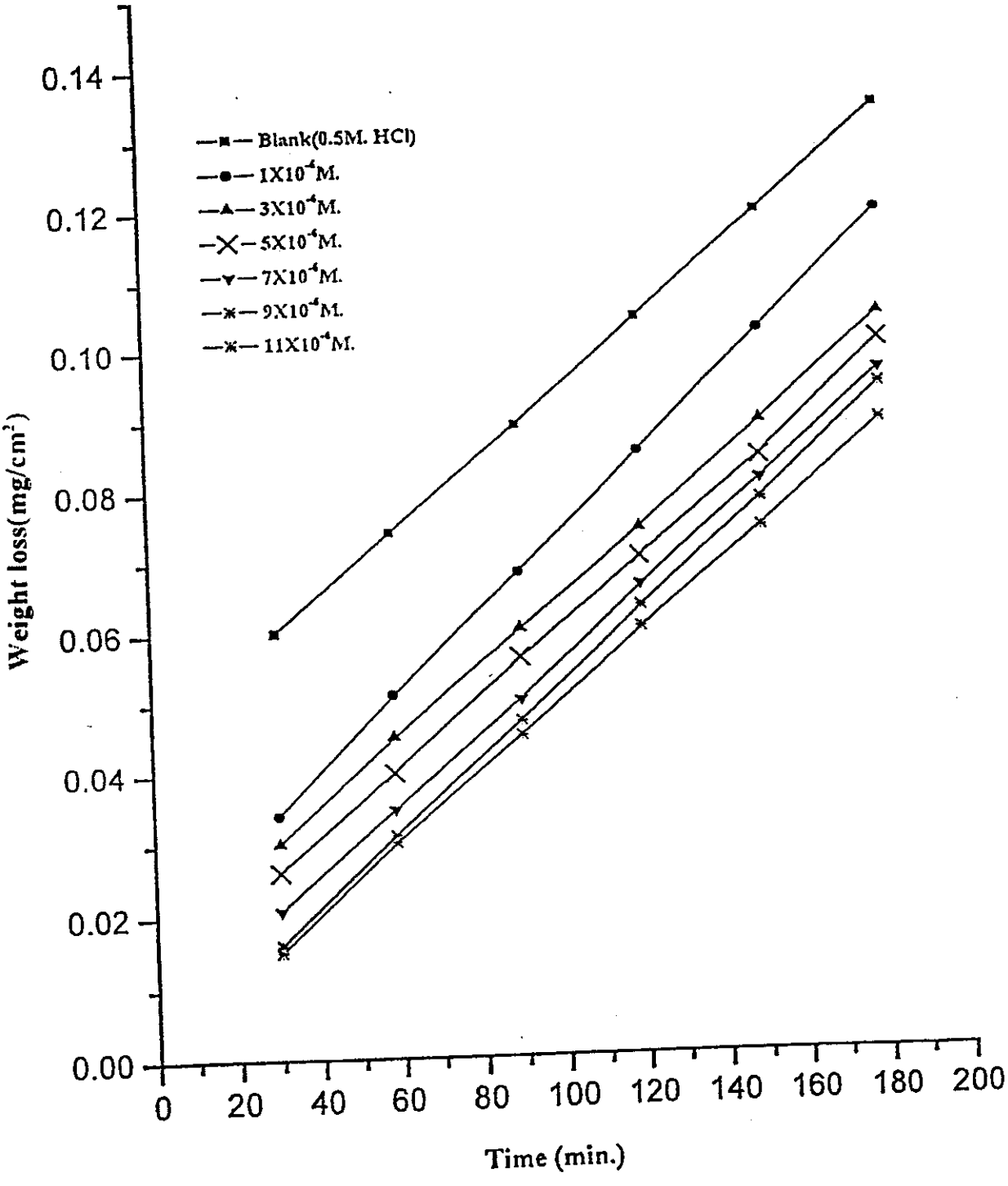

Fig. (3.16) Weight loss - time curves for corrosion of arsenic in presence and absence of different concentrations of compound (a) at 30° C.

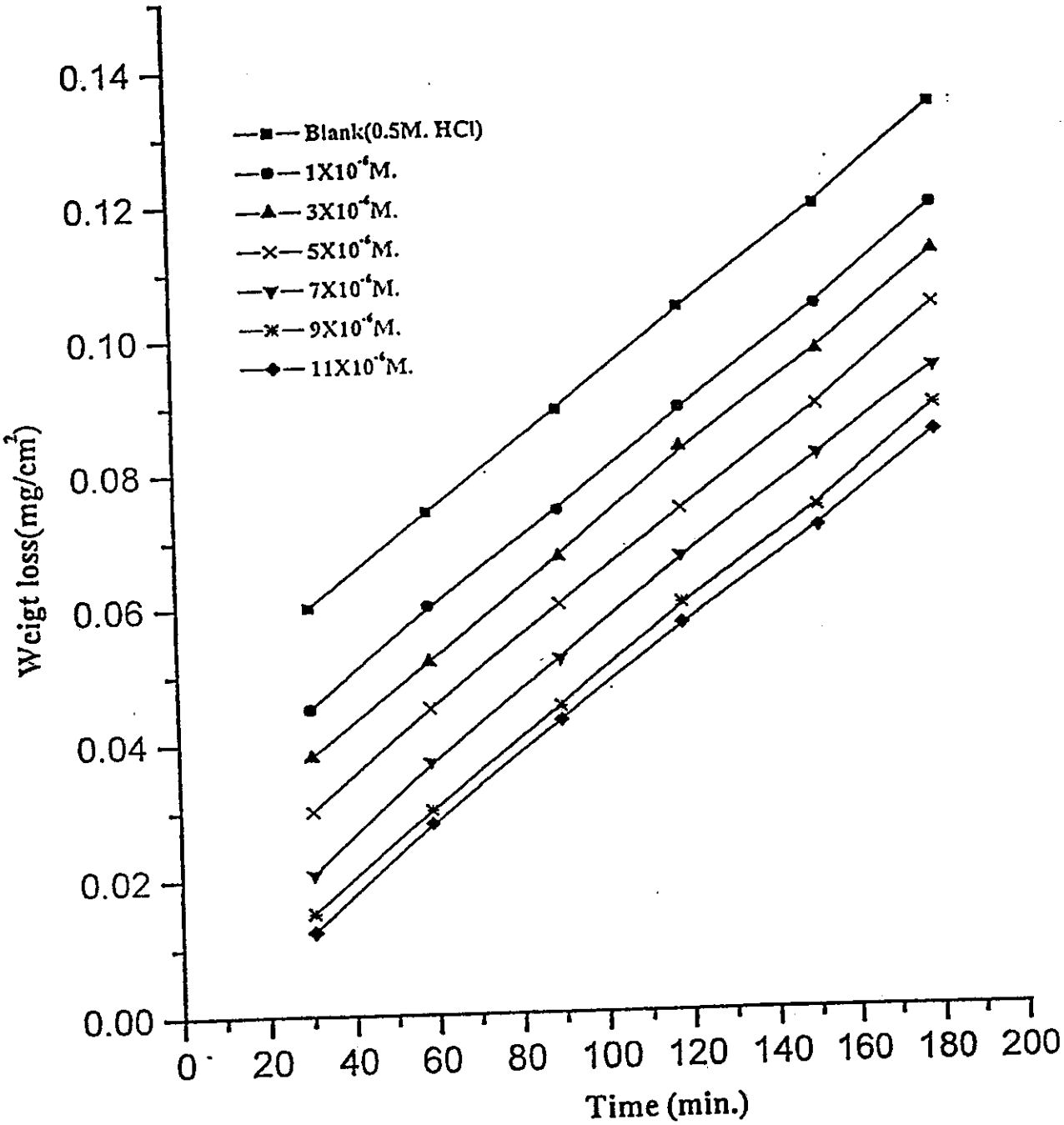

Fig. (3.17) Weight loss - time curves for corrosion of arsenic in presence and absence of different concentrations of compound (b) at 30° C.

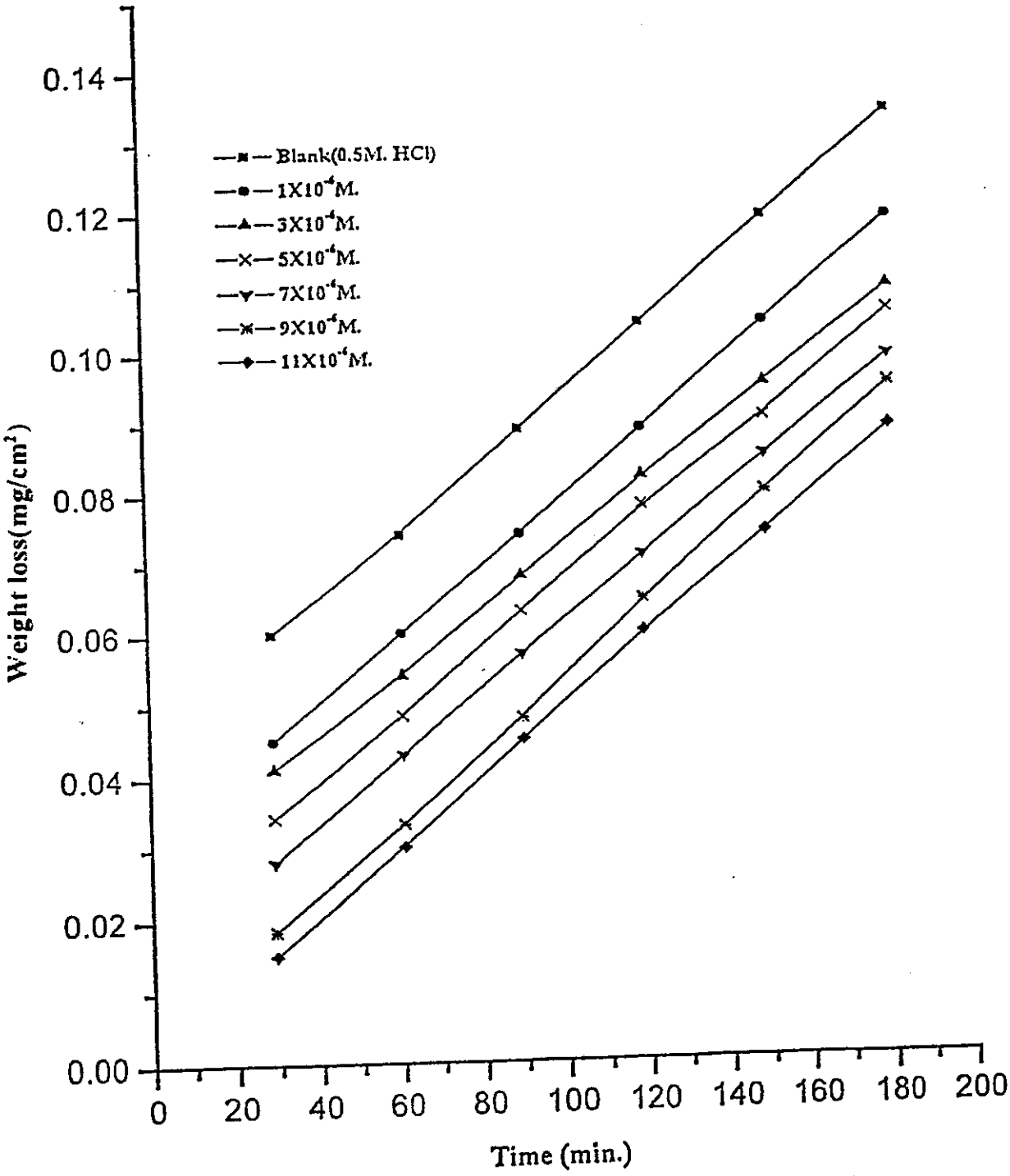

Fig. (3.18) Weight loss - time curves for corrosion of arsenic in presence and absence of different concentrations of compound (c) at 30° C.

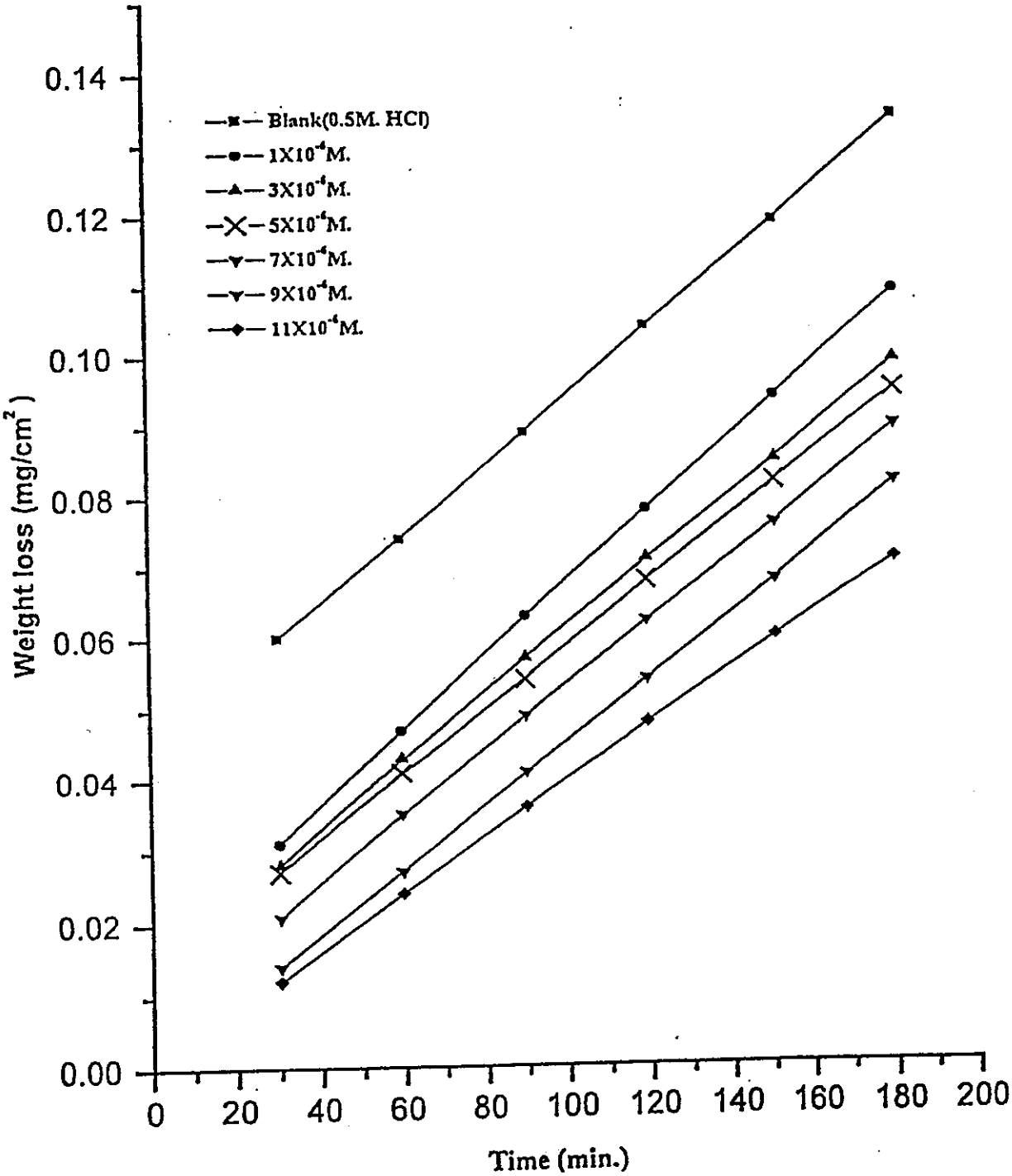

Fig. (3.19) Weight loss - time curves for corrosion of arsenic in presence and absence of different concentrations of compound (d) at 30° C.

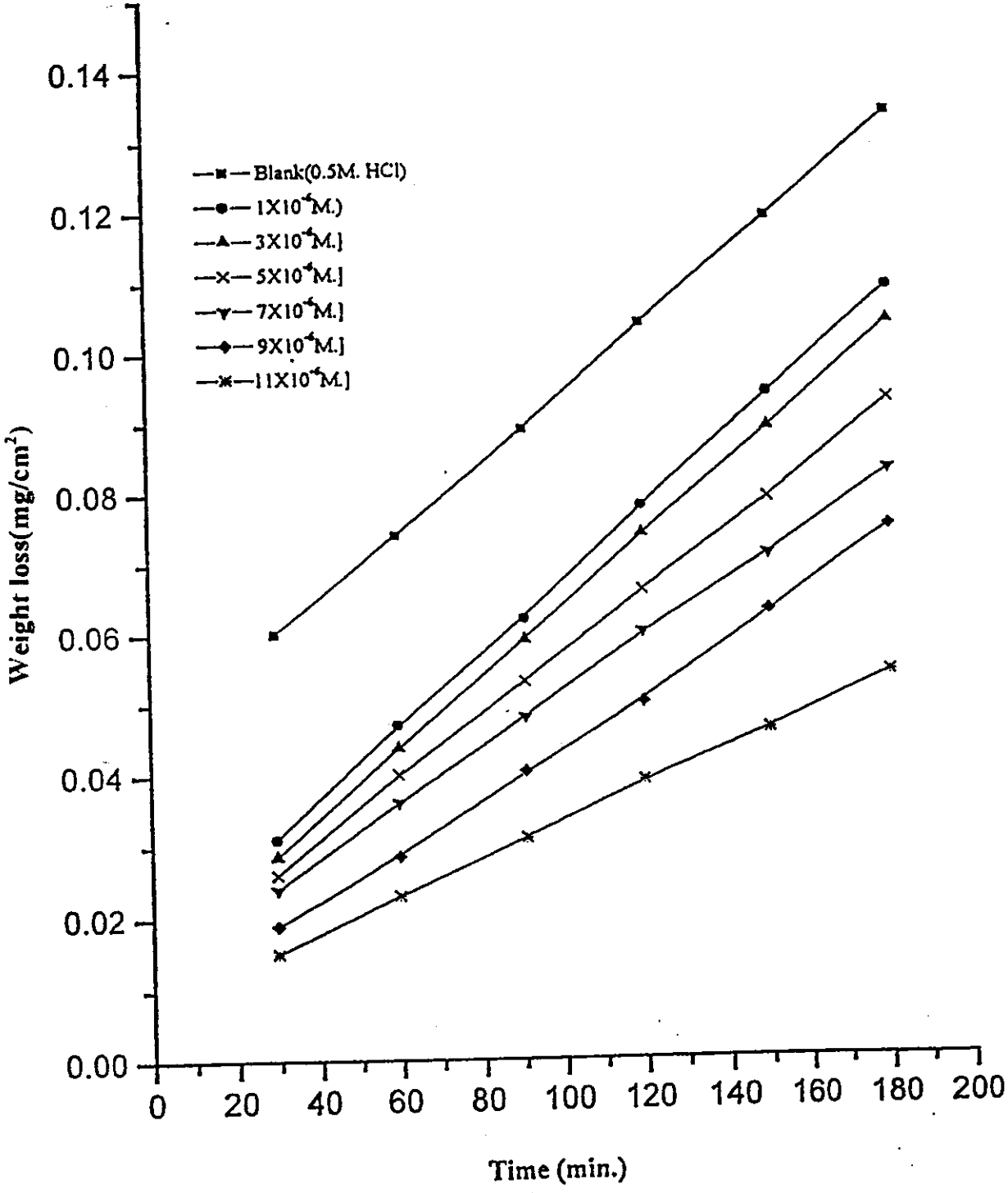

Fig. (3.20) Weight loss - time curves for corrosion of arsenic in presence and absence of different concentrations of compound (e) at 30° C.

3.2- GALVANOSTATIC POLARIZATION MESUREMENTS

Both anodic and cathodic polarization of copper in 0.5M HCl in absence and presence of different concentrations of benzylideneaniline derivatives are shown in Figs. (3.21 - 3.40). It is found that polarization behaviour for alloys of copper in the media follows almost the similar pattern. Various corrosion kinetic parameters such as corrosion potential ($E_{corr.}$), corrosion current ($i_{corr.}$), and Tafel slopes β_a and β_c derived from the above polarization curves are given in Tables (3.6 – 3.25).

It can be seen from these tables that all these compounds function as corrosion inhibitors, in 0.5M HCl. They behave as mixed – type inhibitors, but the cathode is more polarized when an external current density was applied ($\beta_c > \beta_a$).

The efficiency of the benzylideneaniline derivatives as corrosion inhibitors for copper and its alloys in 0.5M HCl depends upon their nature, their concentrations and the type of the alloy. The order of increasing inhibition efficiency of these derivatives at most concentrations is [Tables (3.26-3.29)]: $b < c < a < d < e$ and the extent of copper corrosion and its alloys in 0.5M HCl follows the order [Tables (3.26-3.29)]: Muntz alloy > admiralty brass > copper > arsenic.

Table (3.6). The effect of compound (a) concentrations on the free corrosion potential ($E_{corr.}$), corrosion current density ($i_{corr.}$), Tafel slopes (β_a & β_c), inhibition efficiency (Pi) and degree of surface coverage (θ) of muntz in 0.5M HCl at 30°C.

Concentration (M)	$-E_{corr.}$ (mV)	$i_{corr.}$ ($\mu A/cm^2$)	β_a mV/current decade	β_c mV/current decade	$\%P_i$	θ
0	356	14.8	90	148	-	-
$1x10^{-6}$	353	11.7	93	151	21.0	0.21
$3x10^{-6}$	350	9.5	96	153	26.0	0.26
$5x10^{-6}$	347	6.8	99	156	54.0	0.54
$7x10^{-6}$	343	4.3	102	159	71.0	0.71
$9x10^{-6}$	340	2.8	105	162	81.0	0.81
$11x10^{-6}$	336	1.9	108	165	87.0	0.87

Table (3.7). The effect of compound (b) concentrations on the free corrosion potential ($E_{corr.}$), corrosion current density ($i_{corr.}$), Tafel slopes (β_a & β_c), inhibition efficiency (Pi) and degree of surface coverage (θ) of muntz in 0.5M HCl at 30°C.

Concentration (M)	$-E_{corr.}$ (mV)	$i_{corr.}$ ($\mu A/cm^2$)	β_a mV/current decade	β_c mV/current decade	$\%P_i$	θ
0	365	18.6	86	138	-	-
$1x10^{-6}$	362	15.6	88	142	16.0	0.16
$3x10^{-6}$	358	12.8	90	146	31.0	0.31
$5x10^{-6}$	354	9.2	93	150	50.0	0.50
$7x10^{-6}$	351	6.3	95	156	66.0	0.66
$9x10^{-6}$	347	4.0	97	160	78.0	0.78
$11x10^{-6}$	343	2.6	99	165	86.0	0.86

Table (3.8). The effect of compound (c) concentrations on the free corrosion potential ($E_{corr.}$), corrosion current density ($i_{corr.}$), Tafel slopes (β_a & β_c), inhibition efficiency (Pi) and degree of surface coverage (θ) of muntz in 0.5M HCl at 0°C.

Concentration (M)	$-E_{corr.}$ (mV)	$i_{corr.}$ ($\mu A/cm^2$)	β_a mV/current decade	β_c mV/current decade	$\%P_i$	θ
0	360	16.6	88	142	-	-
$1x10^{-6}$	357	13.5	90	146	19.0	0.19
$3x10^{-6}$	353	10.9	93	149	34.0	0.34
$5x10^{-6}$	349	8.0	95	153	52.0	0.52
$7x10^{-6}$	345	5.2	98	157	69.0	0.69
$9x10^{-6}$	341	3.5	101	160	79.0	0.79
$11x10^{-6}$	337	2.2	105	165	78.0	0.87

Table (3.9). The effect of compound (d) concentrations on the free corrosion potential ($E_{corr.}$), corrosion current density ($i_{corr.}$), Tafel slopes (β_a & β_c), inhibition efficiency (Pi) and degree of surface coverage (θ) of muntz in 0.5M HCl at 30°C.

Concentration (M)	$-E_{corr.}$ (mV)	$i_{corr.}$ ($\mu A/cm^2$)	β_a mV/current decade	β_c mV/current decade	$\%P_i$	θ
0	353	12.2	92	151	-	-
$1x10^{-6}$	350	9.4	95	153	23.0	0.23
$3x10^{-6}$	347	7.6	97	156	38.0	0.38
$5x10^{-6}$	344	5.2	99	159	57.0	0.57
$7x10^{-6}$	340	3.3	102	162	73.0	0.73
$9x10^{-6}$	336	2.1	105	165	83.0	0.83
$11x10^{-6}$	332	1.5	108	169	88.0	0.88

Table (3.10). The effect of compound (e) concentrations on the free corrosion potential ($E_{corr.}$), corrosion current density ($i_{corr.}$), Tafel slopes (β_a & β_c), inhibition efficiency (Pi) and degree of surface coverage (θ) of muntz in 0.5M HCl at 30°C.

Concentration (M)	$-E_{corr.}$ (mV)	$i_{corr.}$ ($\mu A/cm^2$)	β_a mV/current decade	β_c mV/current decade	$\%P_i$	θ
0	350	11.0	94	154	-	-
$1x10^{-6}$	347	8.2	97	158	25.0	0.25
$3x10^{-6}$	344	6.6	99	162	40.0	0.40
$5x10^{-6}$	341	4.2	101	165	61.0	0.61
$7x10^{-6}$	338	2.5	103	169	77.0	0.77
$9x10^{-6}$	334	1.8	105	173	84.0	0.84
$11x10^{-6}$	332	1.2	108	178	89.0	0.89

Table (3.11). The effect of compound (a) concentrations on the free corrosion potential ($E_{corr.}$), corrosion current density ($i_{corr.}$), Tafel slopes (β_a & β_c), inhibition efficiency (Pi) and degree of surface coverage (θ) of admiralty in 0.5M HCl at 30°C.

Concentration (M)	$-E_{corr.}$ (mV)	$i_{corr.}$ ($\mu A/cm^2$)	β_a mV/current decade	β_c mV/current decade	$\%P_i$	θ
0	377	13.5	92	146	-	-
$1x10^{-6}$	374	10.8	94	149	20.0	0.20
$3x10^{-6}$	370	8.9	96	154	34.0	0.34
$5x10^{-6}$	366	6.4	99	158	53.0	0.53
$7x10^{-6}$	361	4.1	102	162	70.0	0.70
$9x10^{-6}$	357	2.5	105	166	81.0	0.81
$11x10^{-6}$	353	1.6	108	170	88.0	0.88

Table (3.12). The effect of compound (b) concentrations on the free corrosion potential ($E_{corr.}$), corrosion current density ($i_{corr.}$), Tafel slopes (β_a & β_c), inhibition efficiency (Pi) and degree of surface coverage (θ) of admiralty in 0.5M HCl at 30°C.

Concentration (M)	$-E_{corr.}$ (mV)	$i_{corr.}$ ($\mu A/cm^2$)	β_a mV/current decade	β_c mV/current decade	$\%P_i$	θ
0	385	20	88	138	-	-
$1x10^{-6}$	382	16.5	90	142	18.0	0.18
$3x10^{-6}$	378	13.6	92	146	32.0	0.32
$5x10^{-6}$	374	9.9	95	150	51.0	0.51
$7x10^{-6}$	370	6.6	97	155	67.0	0.67
$9x10^{-6}$	367	4.2	100	160	79.0	0.79
$11x10^{-6}$	362	2.8	104	165	86.0	0.86

Table (3.13). The effect of compound (c) concentrations on the free corrosion potential ($E_{corr.}$), corrosion current density ($i_{corr.}$), Tafel slopes (β_a & β_c), inhibition efficiency (Pi) and degree of surface coverage (θ) of admiralty in 0.5M HCl at 30°C.

Concentration (M)	$-E_{corr.}$ (mV)	$i_{corr.}$ ($\mu A/cm^2$)	β_a mV/current decade	β_c mV/current decade	$\%P_i$	θ
0	380	17	90	142	-	-
$1x10^{-6}$	377	13.7	92	146	19.0	0.19
$3x10^{-6}$	374	11.4	95	150	33.0	0.33
$5x10^{-6}$	370	8.2	97	156	52.0	0.52
$7x10^{-6}$	366	5.5	99	160	68.0	0.68
$9x10^{-6}$	362	3.4	101	164	80.0	0.80
$11x10^{-6}$	358	2.2	104	169	87.0	0.87

Table (3.14). The effect of compound (d) concentrations on the free corrosion potential ($E_{corr.}$), corrosion current density ($i_{corr.}$), Tafel slopes (β_a & β_c), inhibition efficiency (Pi) and degree of surface coverage (θ) of admiralty in 0.5M HCl at 30°C.

Concentration (M)	$-E_{corr.}$ (mV)	$i_{corr.}$ ($\mu A/cm^2$)	β_a mV/current decade	β_c mV/current decade	$\%P_i$	θ
0	373	11.6	94	149	-	-
$1x10^{-6}$	370	9.2	96	153	21.0	0.21
$3x10^{-6}$	367	7.5	99	156	35.0	0.35
$5x10^{-6}$	363	5.3	102	161	54.0	0.54
$7x10^{-6}$	359	3.2	105	165	72.0	0.72
$9x10^{-6}$	355	2.1	107	169	82.0	0.82
$11x10^{-6}$	352	1.3	109	173	89.0	0.89

Table (3.15). The effect of compound (e) concentrations on the free corrosion potential ($E_{corr.}$), corrosion current density ($i_{corr.}$), Tafel slopes (β_a & β_c), inhibition efficiency (Pi) and degree of surface coverage (θ) of admiralty in 0.5M HCl at 30°C.

Concentration (M)	$-E_{corr.}$ (mV)	$i_{corr.}$ ($\mu A/cm^2$)	β_a mV/current decade	β_c mV/current decade	$\%P_i$	θ
0	370	10.8	96	152	-	-
$1x10^{-6}$	367	8.4	99	155	22.0	0.22
$3x10^{-6}$	364	6.9	103	159	36.0	0.36
$5x10^{-6}$	361	4.7	106	163	56.0	0.56
$7x10^{-6}$	357	2.8	109	167	74.0	0.74
$9x10^{-6}$	353	1.8	112	170	83.0	0.83
$11x10^{-6}$	350	1.1	114	174	90.0	0.90

Table (3.16). The effect of compound (a) concentrations on the free corrosion potential ($E_{corr.}$), corrosion current density ($i_{corr.}$), Tafel slopes (β_a & β_c), inhibition efficiency (Pi) and degree of surface coverage (θ) of copper in 0.5M HCl at 30°C.

Concentration (M)	$-E_{corr.}$ (mV)	$i_{corr.}$ ($\mu A/cm^2$)	β_a mV/current decade	β_c mV/current decade	$\%P_i$	θ
0	262	13.5	75	221	-	-
$1x10^{-6}$	259	11.0	79	224	19.0	0.19
$3x10^{-6}$	254	8.9	83	228	34.0	0.34
$5x10^{-6}$	250	6.1	86	231	55.0	0.55
$7x10^{-6}$	246	3.4	90	235	75.0	0.75
$9x10^{-6}$	241	2.1	93	239	84.0	0.84
$11x10^{-6}$	238	1.1	95	243	92.0	0.92

Table (3.17). The effect of compound (b) concentrations on the free corrosion potential ($E_{corr.}$), corrosion current density ($i_{corr.}$), Tafel slopes (β_a & β_c), inhibition efficiency (Pi) and degree of surface coverage (θ) of copper in 0.5M HCl at 30°C.

Concentration (M)	$-E_{corr.}$ (mV)	$i_{corr.}$ ($\mu A/cm^2$)	β_a mV/current decade	β_c mV/current decade	$\%P_i$	θ
0	276	18.0	68	214	-	-
$1x10^{-6}$	273	15.2	72	218	16.0	0.16
$3x10^{-6}$	270	12.3	74	223	32.0	0.32
$5x10^{-6}$	267	8.2	77	230	54.0	0.54
$7x10^{-6}$	264	5.1	79	237	72.0	0.72
$9x10^{-6}$	261	3.2	82	242	82.0	0.82
$11x10^{-6}$	258	1.8	85	249	90.0	0.90

Table (3.19). The effect of compound (d) concentrations on the free corrosion potential ($E_{corr.}$), corrosion current density ($i_{corr.}$), Tafel slopes (β_a & β_c), inhibition efficiency (Pi) and degree of surface coverage (θ) of copper in 0.5M HCl at 30°C.

Concentration (M)	$-E_{corr.}$ (mV)	$i_{corr.}$ ($\mu A/cm^2$)	β_a mV/current decade	β_c mV/current decade	$\%P_i$	θ
0	256	12.2	78	224	-	-
$1x10^{-6}$	253	9.8	81	228	20.0	0.20
$3x10^{-6}$	250	7.8	84	232	36.0	0.36
$5x10^{-6}$	246	5.0	88	236	59.0	0.59
$7x10^{-6}$	242	2.8	90	239	77.0	0.77
$9x10^{-6}$	238	1.7	93	243	86.0	0.86
$11x10^{-6}$	235	0.8	96	246	93.0	0.93

Table (3.21). The effect of compound (a) concentrations on the free corrosion potential ($E_{corr.}$), corrosion current density ($i_{corr.}$), Tafel slopes (β_a & β_c), inhibition efficiency (Pi) and degree of surface coverage (θ) of arsenic in 0.5M HCl at 30°C.

Concentration (M)	$-E_{corr.}$ (mV)	$i_{corr.}$ ($\mu A/cm^2$)	β_a mV/current decade	β_c mV/current decade	$\%P_i$	θ
0	262	10	86	137	-	-
$1x10^{-6}$	260	8.0	89	141	20.0	0.20
$3x10^{-6}$	257	6.5	92	145	35.0	0.35
$5x10^{-6}$	254	4.6	95	149	54.0	0.54
$7x10^{-6}$	251	3.0	98	154	70.0	0.70
$9x10^{-6}$	248	1.8	101	158	82.0	0.82
$11x10^{-6}$	245	1.3	104	162	87.0	0.87

Table (3.22). The effect of compound (b) concentrations on the free corrosion potential ($E_{corr.}$), corrosion current density ($i_{corr.}$), Tafel slopes (β_a & β_c), inhibition efficiency (Pi) and degree of surface coverage (θ) of arsenic in 0.5M HCl at 30°C.

Concentration (M)	$-E_{corr.}$ (mV)	$i_{corr.}$ ($\mu A/cm^2$)	β_a mV/current decade	β_c mV/current decade	$\%P_i$	θ
0	265	14.5	80	128	-	-
$1x10^{-6}$	262	11.7	83	132	19.0	0.19
$3x10^{-6}$	259	9.7	86	136	33.0	0.33
$5x10^{-6}$	255	7.0	89	140	52.0	0.52
$7x10^{-6}$	251	4.6	92	145	68.0	0.68
$9x10^{-6}$	247	2.9	95	150	80.0	0.80
$11x10^{-6}$	243	2.2	98	156	85.0	0.85

Table (3.23). The effect of compound (c) concentrations on the free corrosion potential ($E_{corr.}$), corrosion current density ($i_{corr.}$), Tafel slopes (β_a & β_c), inhibition efficiency (Pi) and degree of surface coverage (θ) of arsenic in 0.5M HCl at 30°C.

Concentration (M)	$-E_{corr.}$ (mV)	$i_{corr.}$ ($\mu A/cm^2$)	β_a mV/current decade	β_c mV/current decade	$\%P_i$	θ
0	268	12.5	83	132	-	-
$1x10^{-6}$	265	10.0	86	136	20.0	0.20
$3x10^{-6}$	262	8.3	89	140	34.0	0.34
$5x10^{-6}$	259	5.9	93	144	53.0	0.53
$7x10^{-6}$	255	3.9	96	149	69.0	0.69
$9x10^{-6}$	251	2.4	99	154	81.0	0.81
$11x10^{-6}$	247	1.8	102	159	86.0	0.86

Table (3.24). The effect of compound (d) concentrations on the free corrosion potential ($E_{corr.}$), corrosion current density ($i_{corr.}$), Tafel slopes (β_a & β_c), inhibition efficiency (Pi) and degree of surface coverage (θ) of arsenic in 0.5M HCl at 30°C.

Concentration (M)	$-E_{corr.}$ (mV)	$i_{corr.}$ ($\mu A/cm^2$)	β_a mV/current decade	β_c mV/current decade	$\%P_i$	θ
0	259	8	90	145	-	-
$1x10^{-6}$	257	6.3	93	150	21.0	0.21
$3x10^{-6}$	255	5.1	96	155	36.0	0.36
$5x10^{-6}$	252	3.6	99	160	55.0	0.55
$7x10^{-6}$	249	2.2	102	165	73.0	0.73
$9x10^{-6}$	246	1.4	105	170	83.0	0.83
$11x10^{-6}$	243	1.0	108	173	88.0	0.88

Table (3.25). The effect of compound (e) concentrations on the free corrosion potential ($E_{corr.}$), corrosion current density ($i_{corr.}$), Tafel slopes (β_a & β_c), inhibition efficiency (Pi) and degree of surface coverage (θ) of arsenic in 0.5M HCl at 30°C.

Concentration (M)	$-E_{corr.}$ (mV)	$i_{corr.}$ ($\mu A/cm^2$)	β_a mV/current decade	β_c mV/current decade	$\%P_i$	θ
0	255	7.2	95	160	-	-
$1x10^{-6}$	252	5.6	98	165	22.0	0.22
$3x10^{-6}$	249	4.5	101	169	38.0	0.38
$5x10^{-6}$	246	3.1	104	173	57.0	0.57
$7x10^{-6}$	243	1.9	107	178	74.0	0.74
$9x10^{-6}$	240	1.1	110	183	85.0	0.85
$11x10^{-6}$	235	0.7	113	186	90.0	0.90

Table (3.26). Variation of the (%) inhibition efficiency for different inhibitors with different concentrations for muntz at 30°C.

Concentration (M)	Percentage inhibition efficiency (% P_i)				
	a	b	C	d	e
$1x10^{-6}$	21	16	19	23	25
$3x10^{-6}$	36	31	34	38	40
$5x10^{-6}$	54	50	52	57	61
$7x10^{-6}$	71	66	69	73	77
$9x10^{-6}$	81	78	79	83	84
$11x10^{-6}$	87	86	87	88	89

Table (3.27). Variation of the (%) inhibition efficiency for different inhibitors with different concentrations for admiralty at 30°C.

Concentration (M)	Percentage inhibition efficiency (% P_i)				
	a	b	c	d	e
$1x10^{-6}$	20	18	19	21	22
$3x10^{-6}$	34	32	33	35	36
$5x10^{-6}$	53	51	52	54	56
$7x10^{-6}$	70	67	68	72	74
$9x10^{-6}$	81	79	80	82	83
$11x10^{-6}$	88	86	87	89	90

Table (3.28). Variation of the (%) inhibition efficiency for different inhibitors with different concentrations for copper at 30°C.

Concentration (M)	Percentage inhibition efficiency (% P_i)				
	a	b	c	d	e
$1x10^{-6}$	19	16	17	20	22
$3x10^{-6}$	34	32	33	36	38
$5x10^{-6}$	55	54	54	59	62
$7x10^{-6}$	75	72	73	77	81
$9x10^{-6}$	84	82	83	86	88
$11x10^{-6}$	92	90	91	93	95

Table (3.29). Variation of the (%) inhibition efficiency for different inhibitors with different concentrations for arsenic at 30°C.

Concentration (M)	Percentage inhibition efficiency (% P_i)				
	a	b	c	d	e
$1x10^{-6}$	20	19	20	21	22
$3x10^{-6}$	35	33	34	36	38
$5x10^{-6}$	54	52	53	55	57
$7x10^{-6}$	70	68	69	73	74
$9x10^{-6}$	82	80	81	83	85
$11x10^{-6}$	87	85	86	88	90

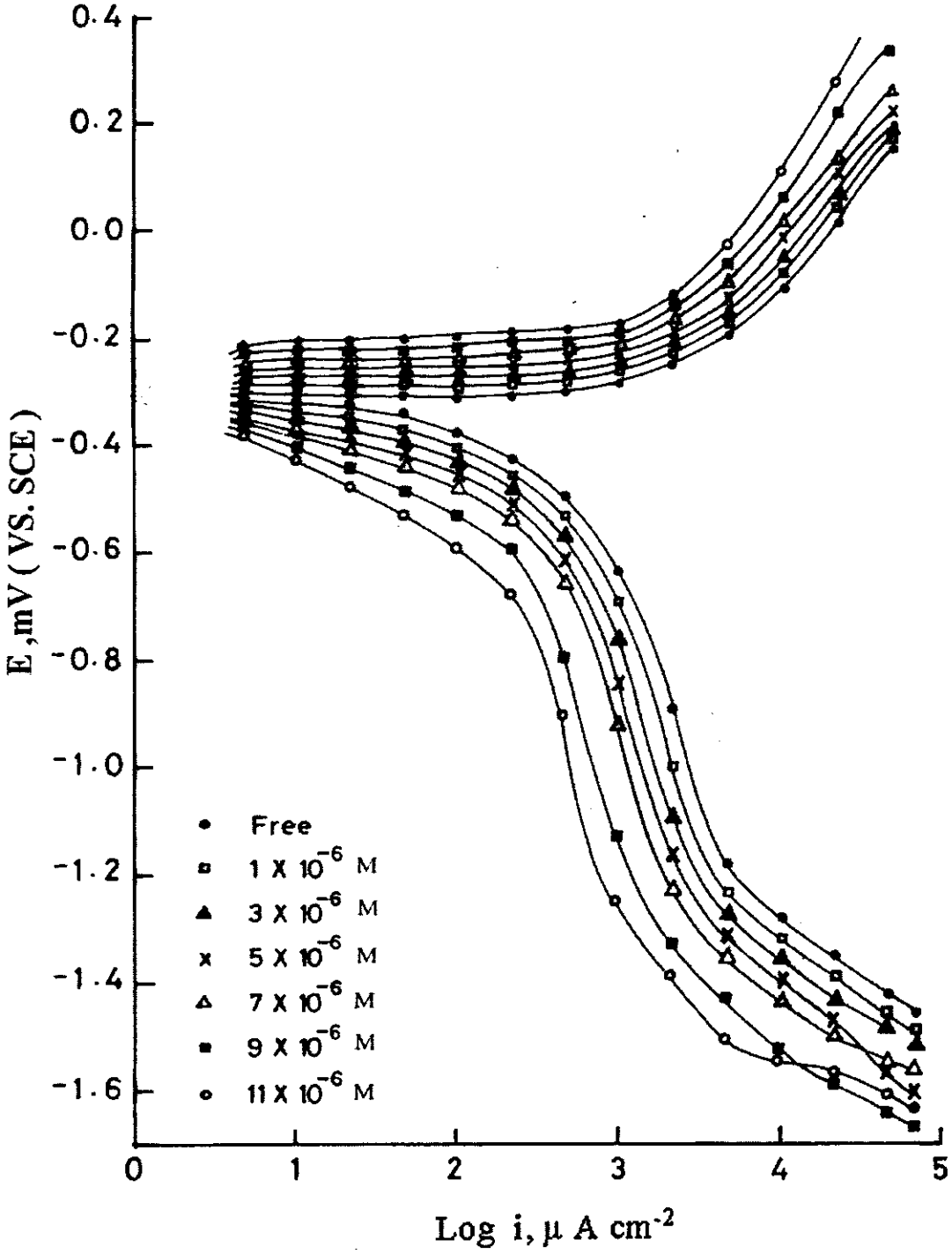

Fig.(3.21): Galvanostatic polarization curves of muntz in 0.5 M HCl alone and containing different concentrations of compound (a).

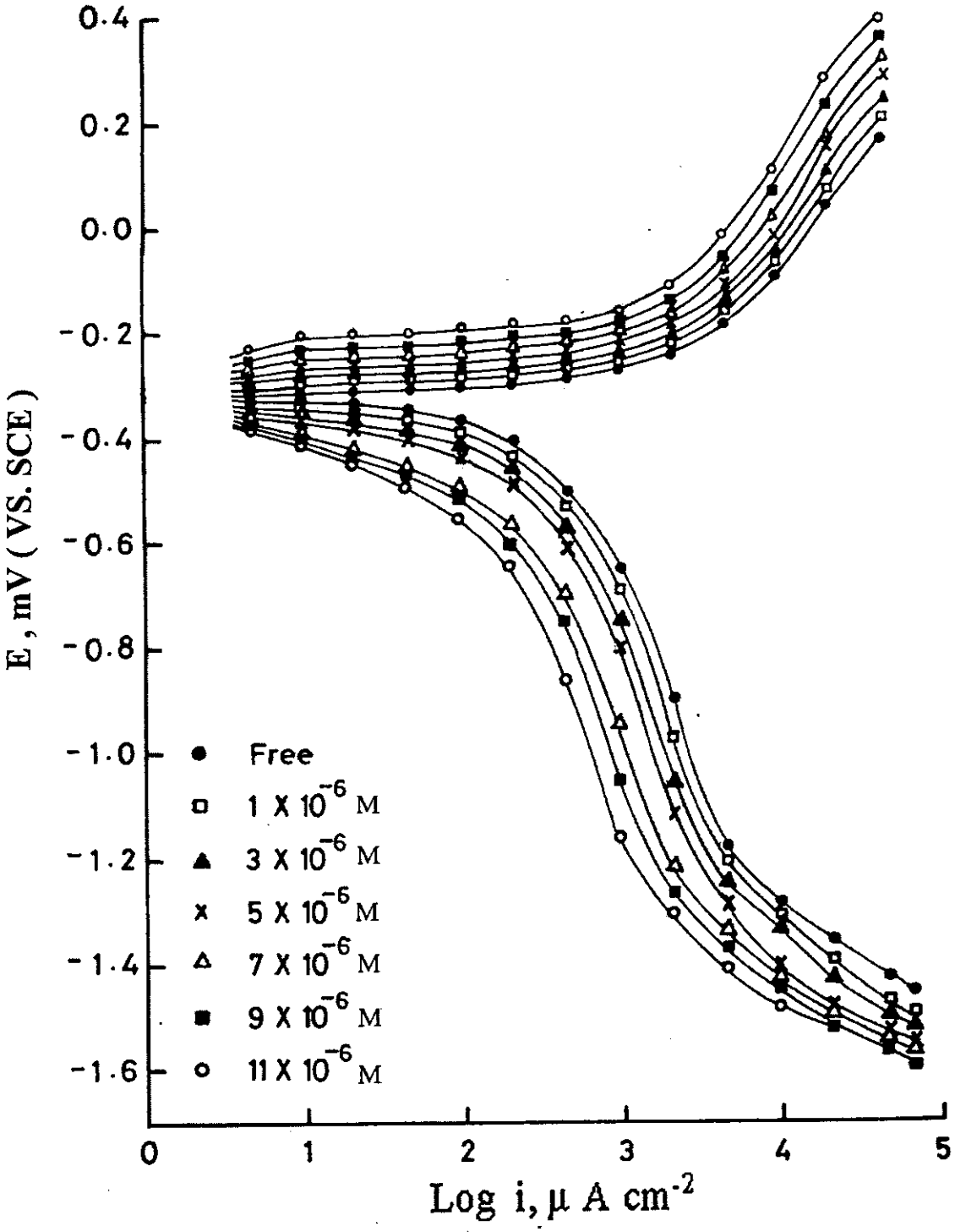

Fig.(3.22): Galvanostatic polarization curves of muntz in 0.5 M HCl alone and containing different concentrations of compound (b).

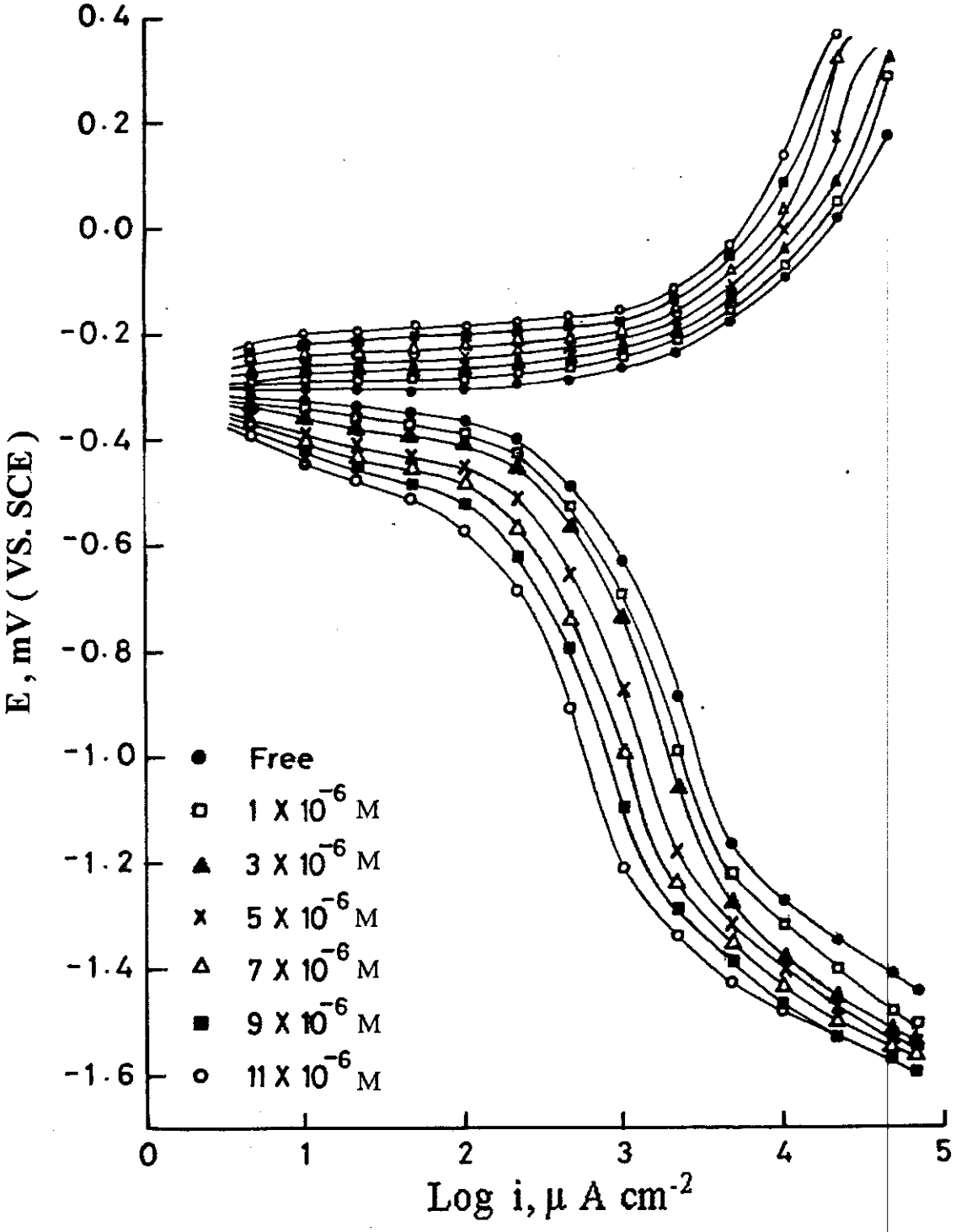

Fig.(3.23): Galvanostatic polarization curves of muntz in 0.5 M HCl alone and containing different concentrations of compound (c).

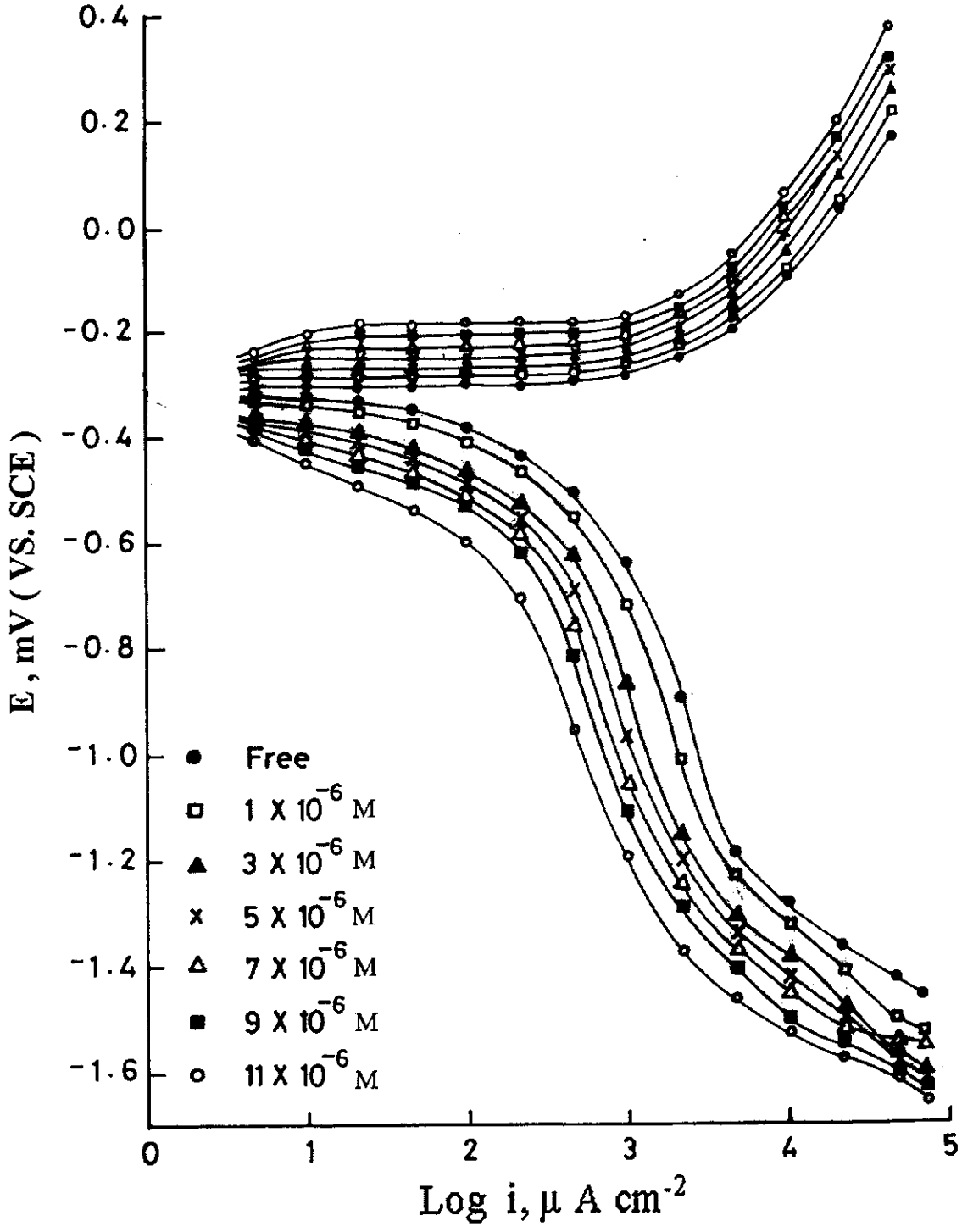

Fig.(3.24): Galvanostatic polarization curves of muntz in 0.5 M HCl alone and containing different concentrations of compound (d).

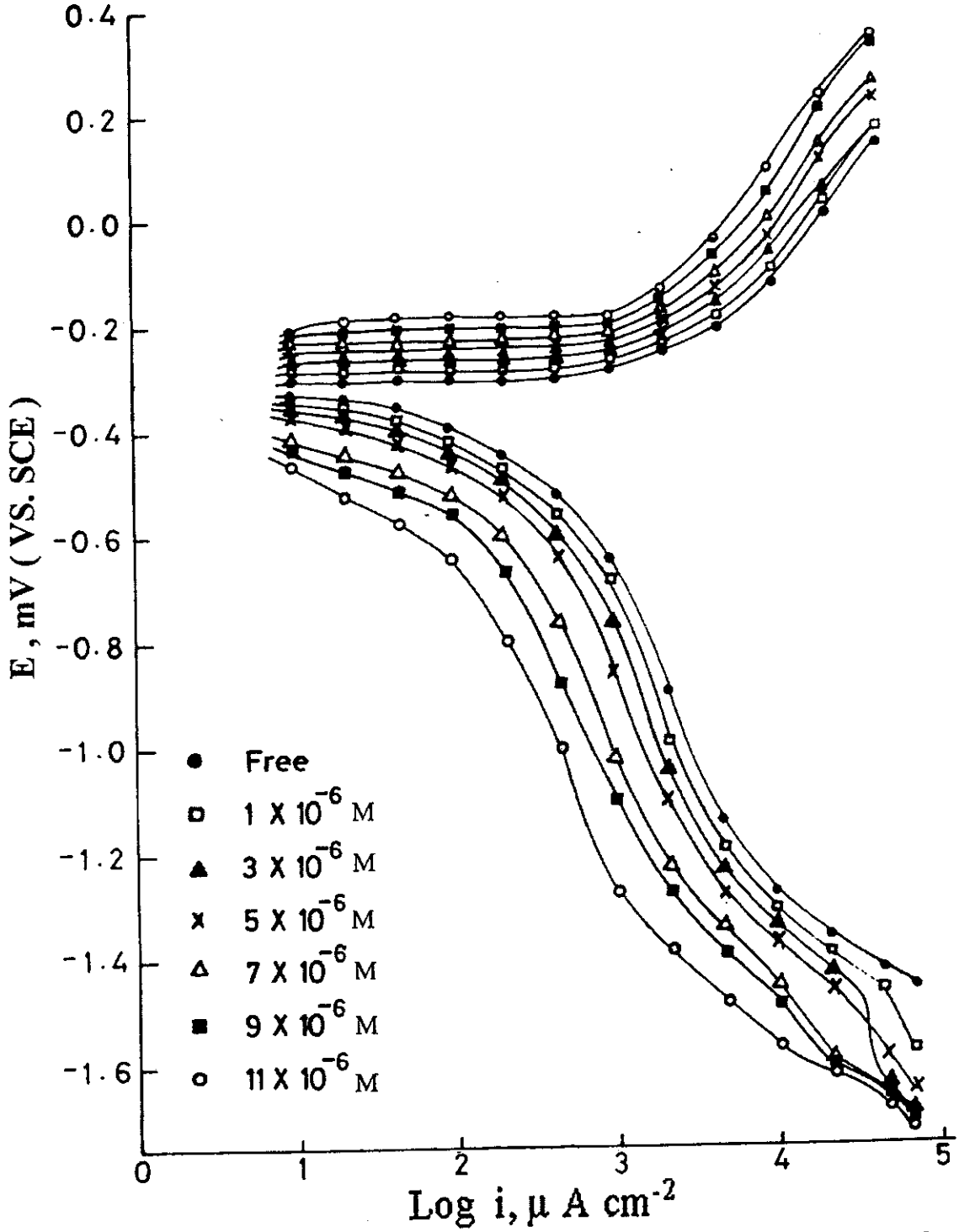

Fig.(3.25): Galvanostatic polarization curves of muntz in 0.5 M HCl alone and containing different concentrations of compound (e).

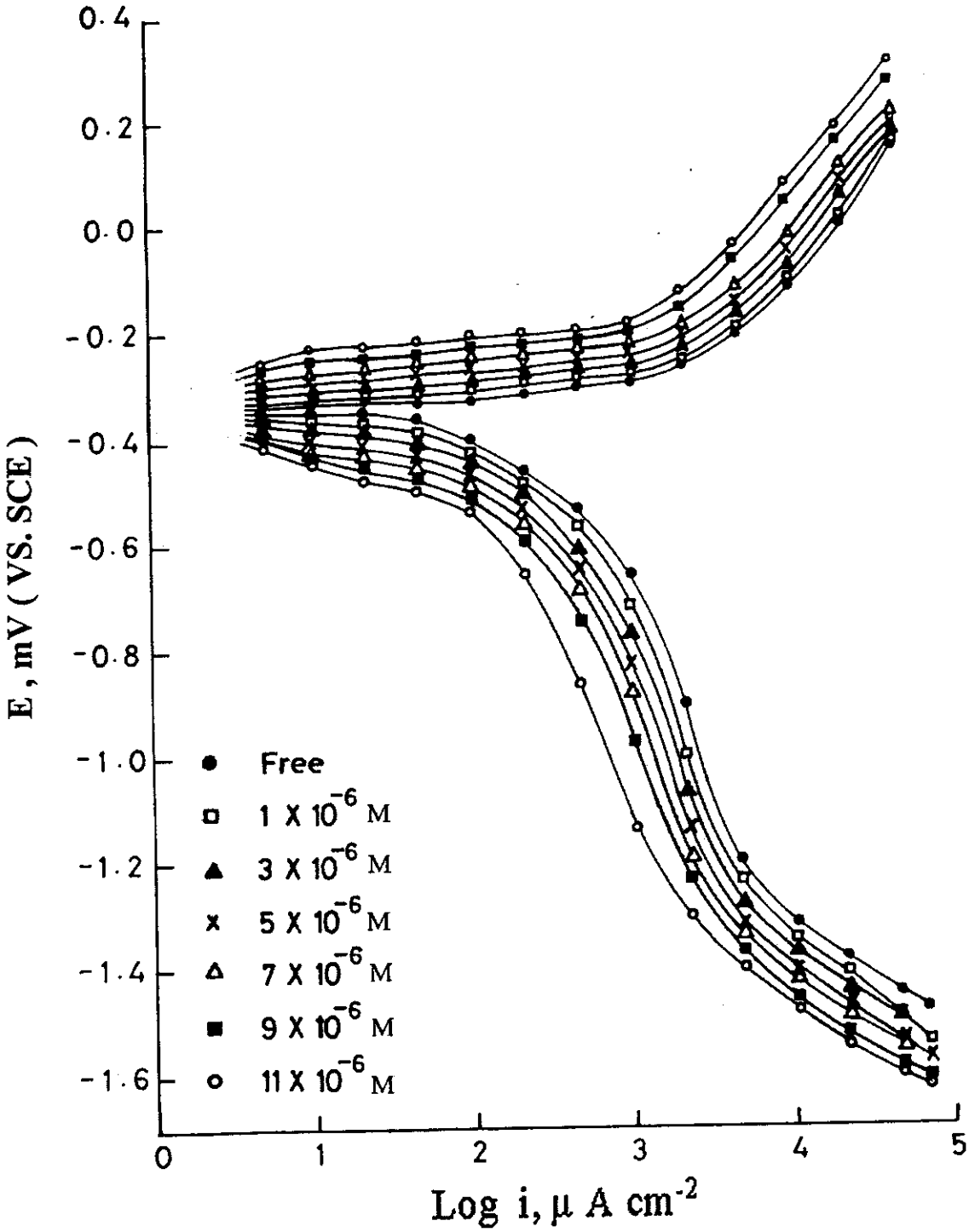

Fig.(3.26): Galvanostatic polarization curves of admiralty in 0.5 M HCl alone and containing different concentrations of compound (a).

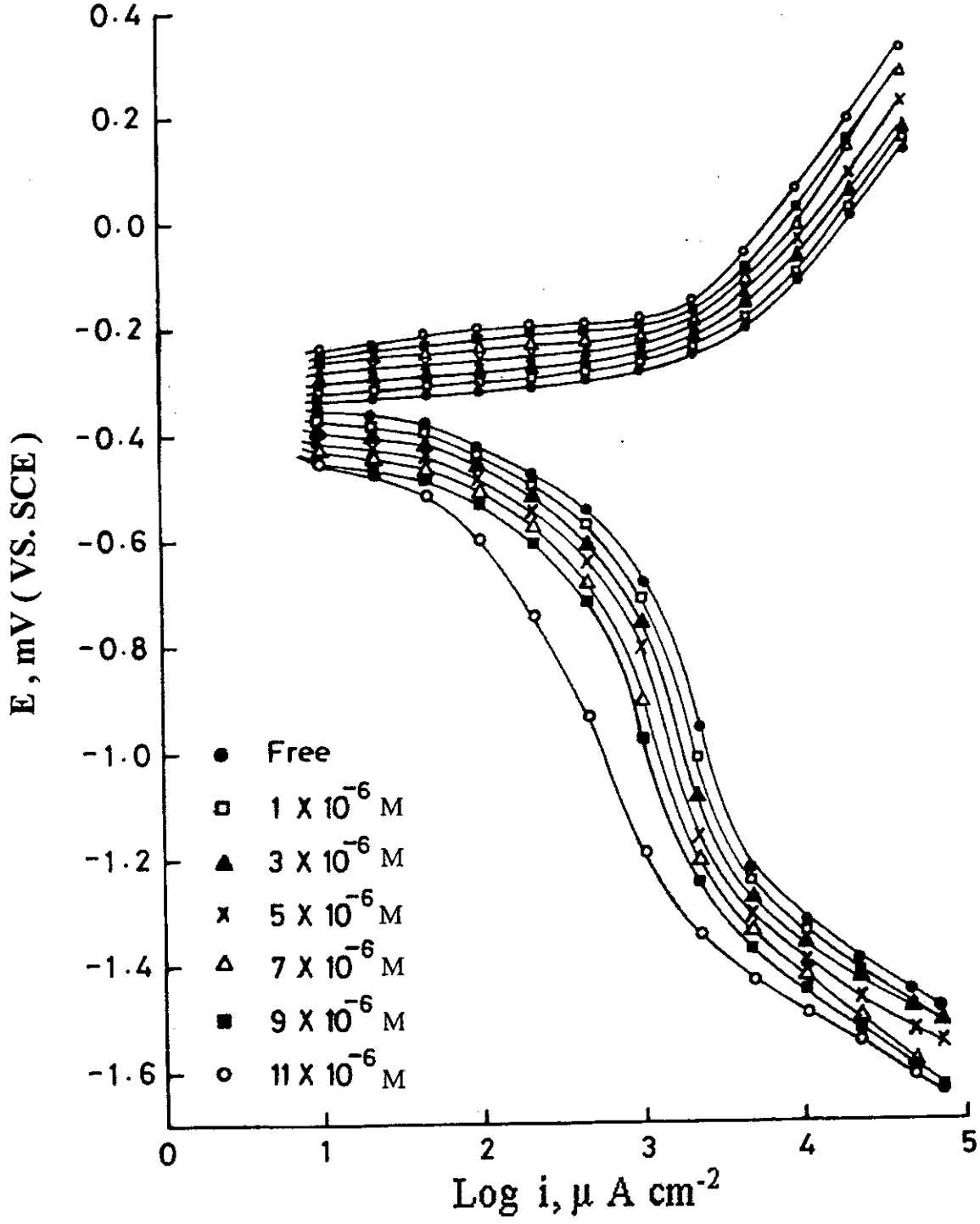

Fig.(3.27): Galvanostatic polarization curves of admiralty in 0.5 M HCl alone and containing different concentrations of compound (b).

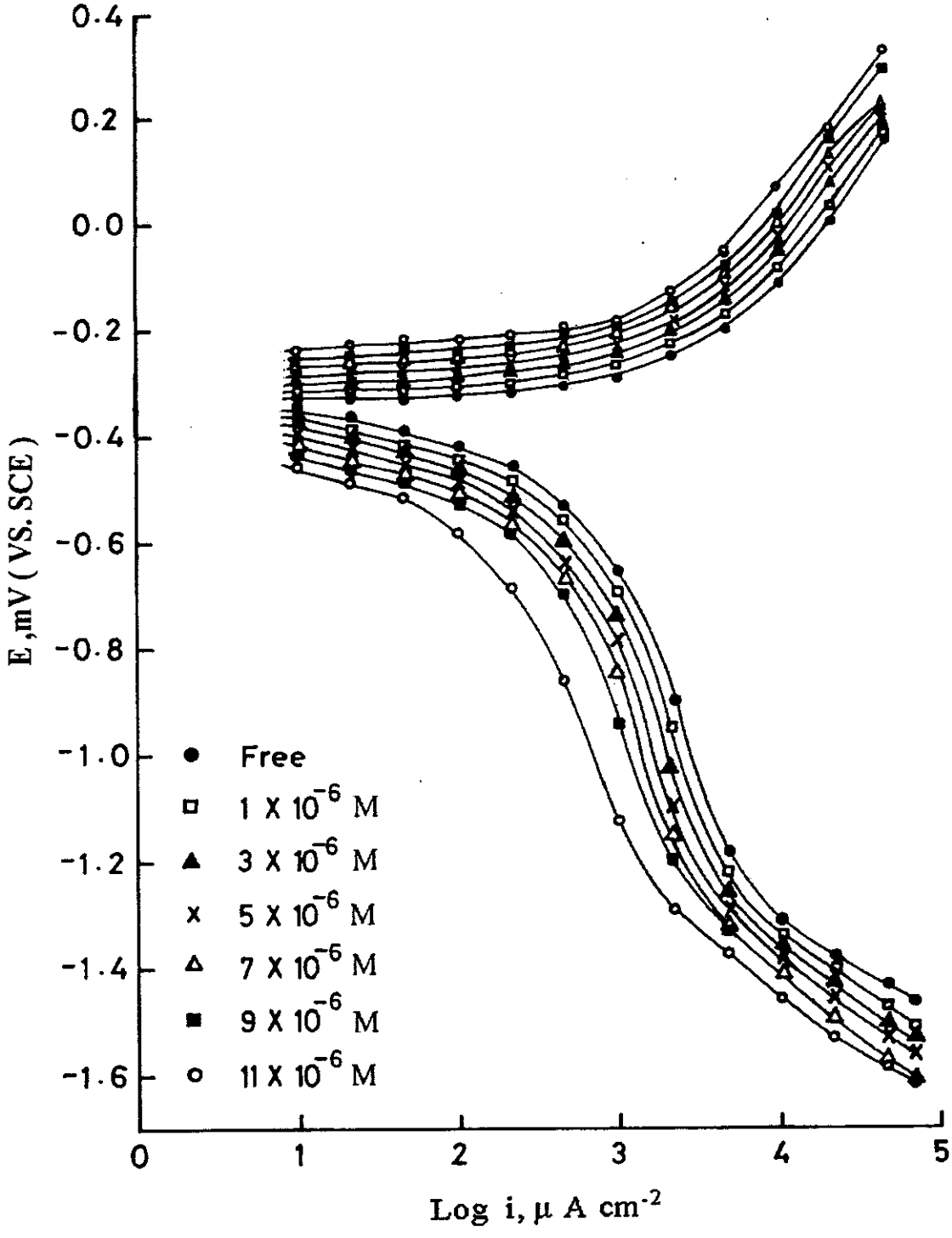

Fig.(3.28): Galvanostatic polarization curves of admiralty in 0.5 M HCl alone and containing different concentrations of compound (c).

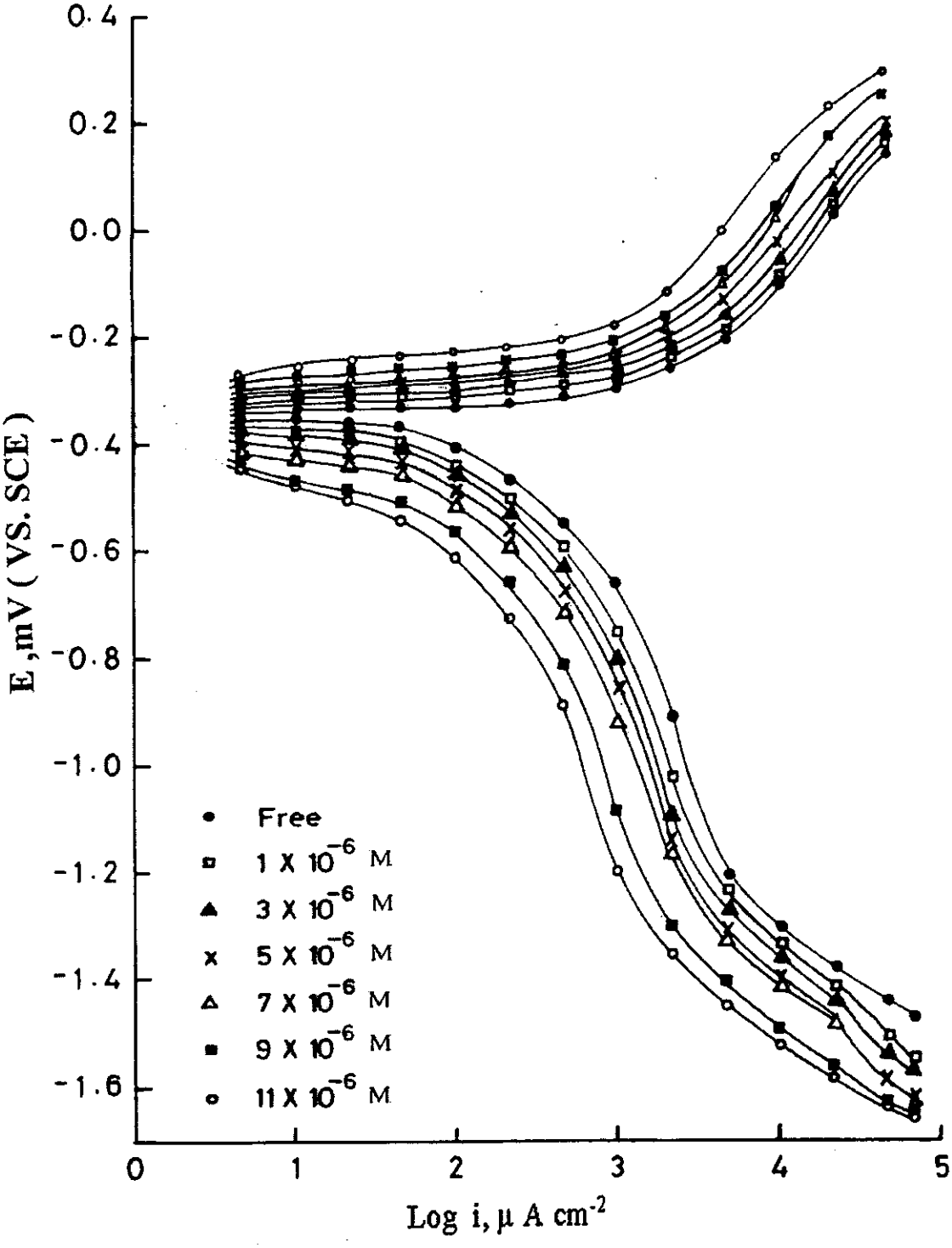

Fig.(3.29): Galvanostatic polarization curves of admiralty in 0·5 M HCl alone and containing different concentrations of compound (d).

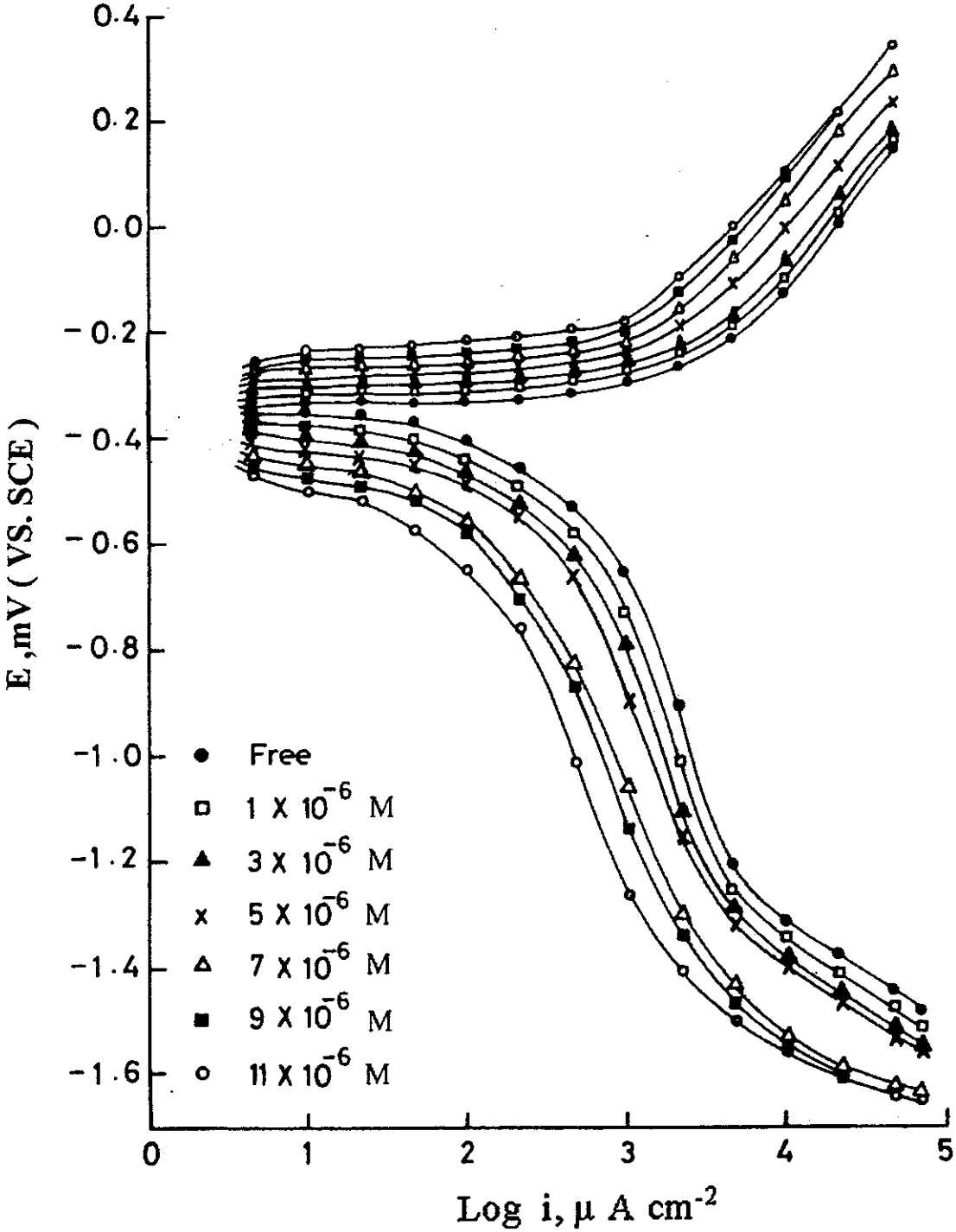

Fig.(3.30): Galvanostatic polarization curves of admiralty in 0.5 M HCl alone and containing different concentrations of compound (e).

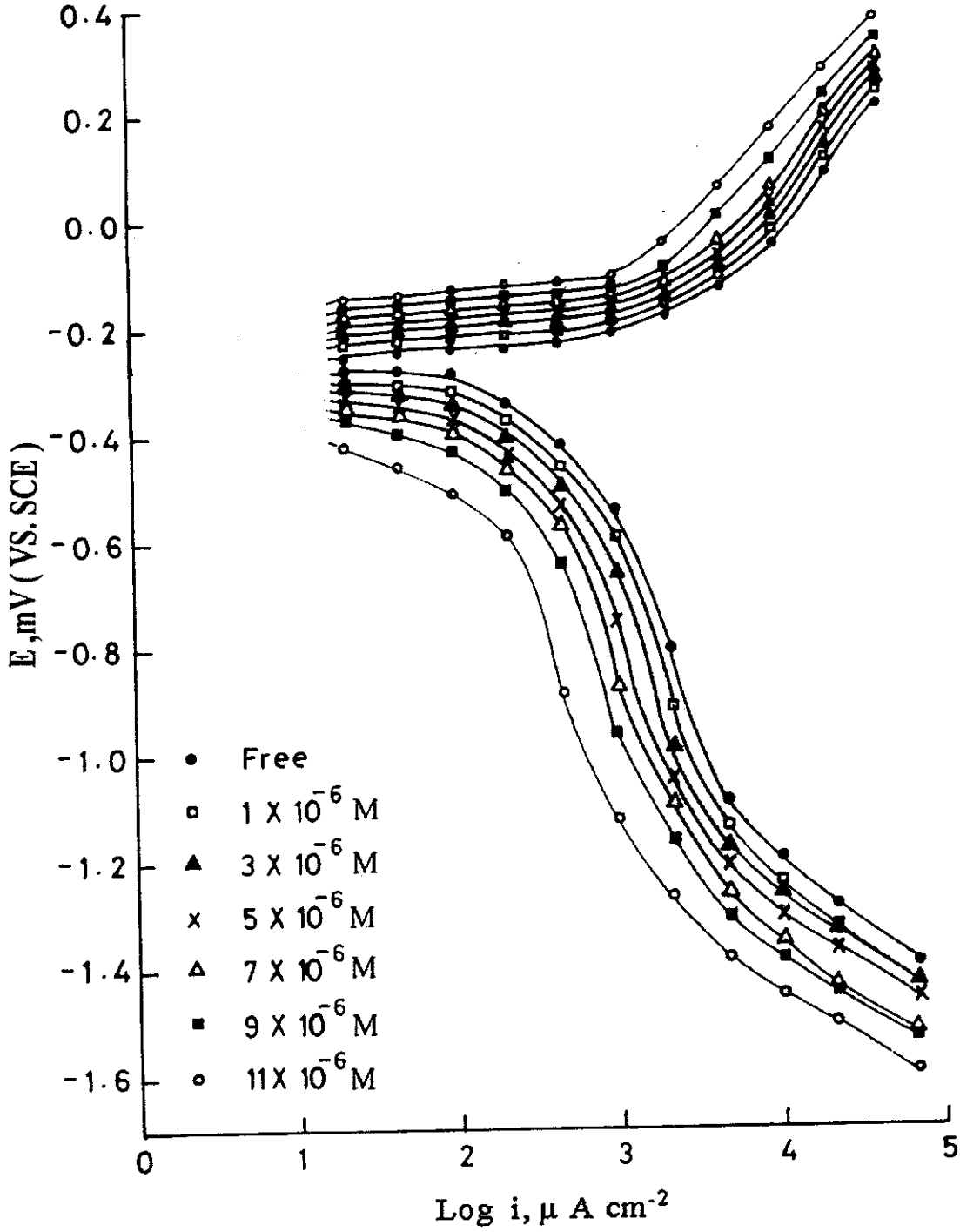

Fig.(3.31): Galvanostatic polarization curves of copper in 0·5 M HCl alone and containing different concentrations of compound (a).

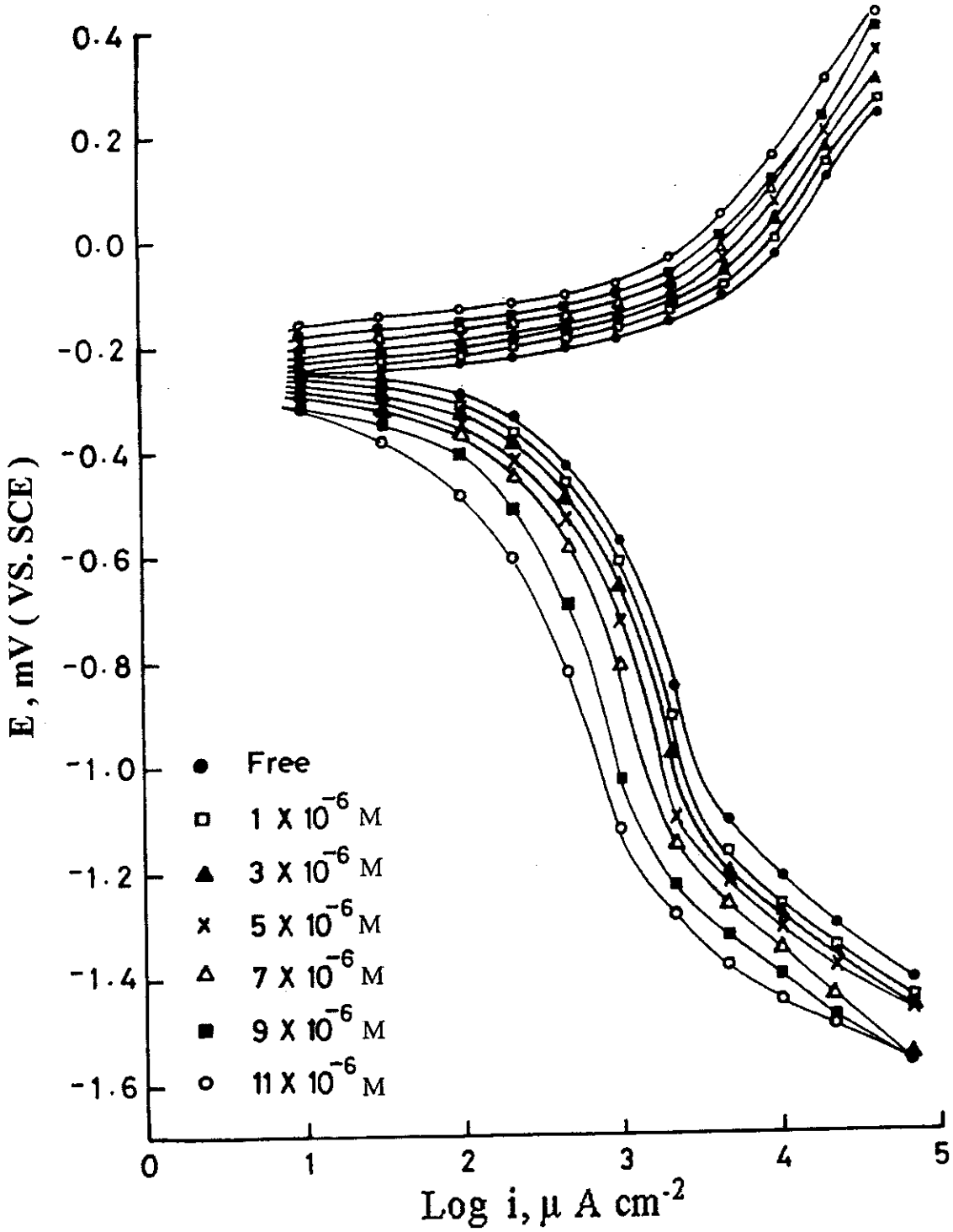

Fig.(3.32): Galvanostatic polarization curves of copper in 0.5 M HCl alone and containing different concentrations of compound (b).

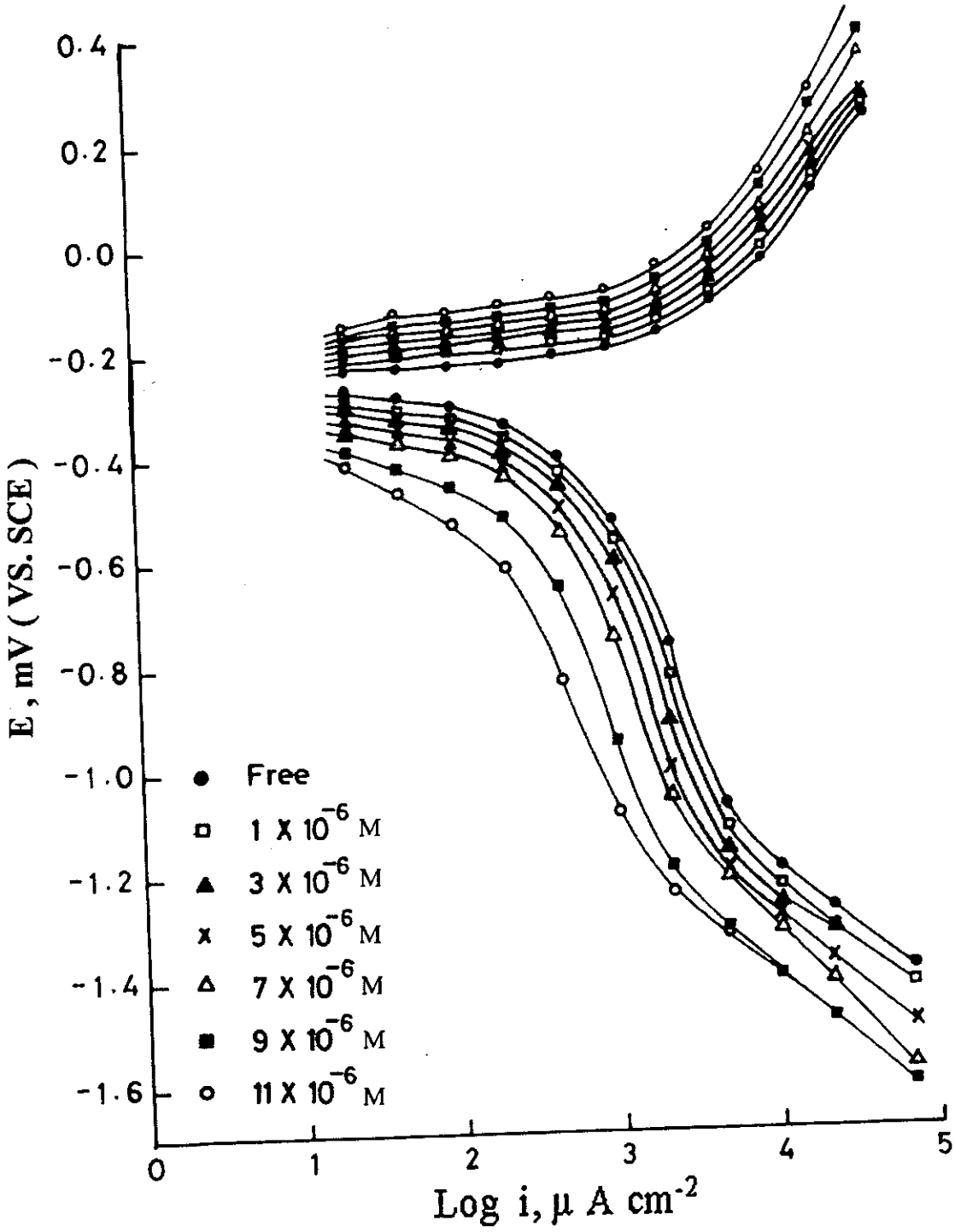

Fig.(3.33): Galvanostatic polarization curves of copper in 0.5 M HCl alone and containing different concentrations of compound (c).

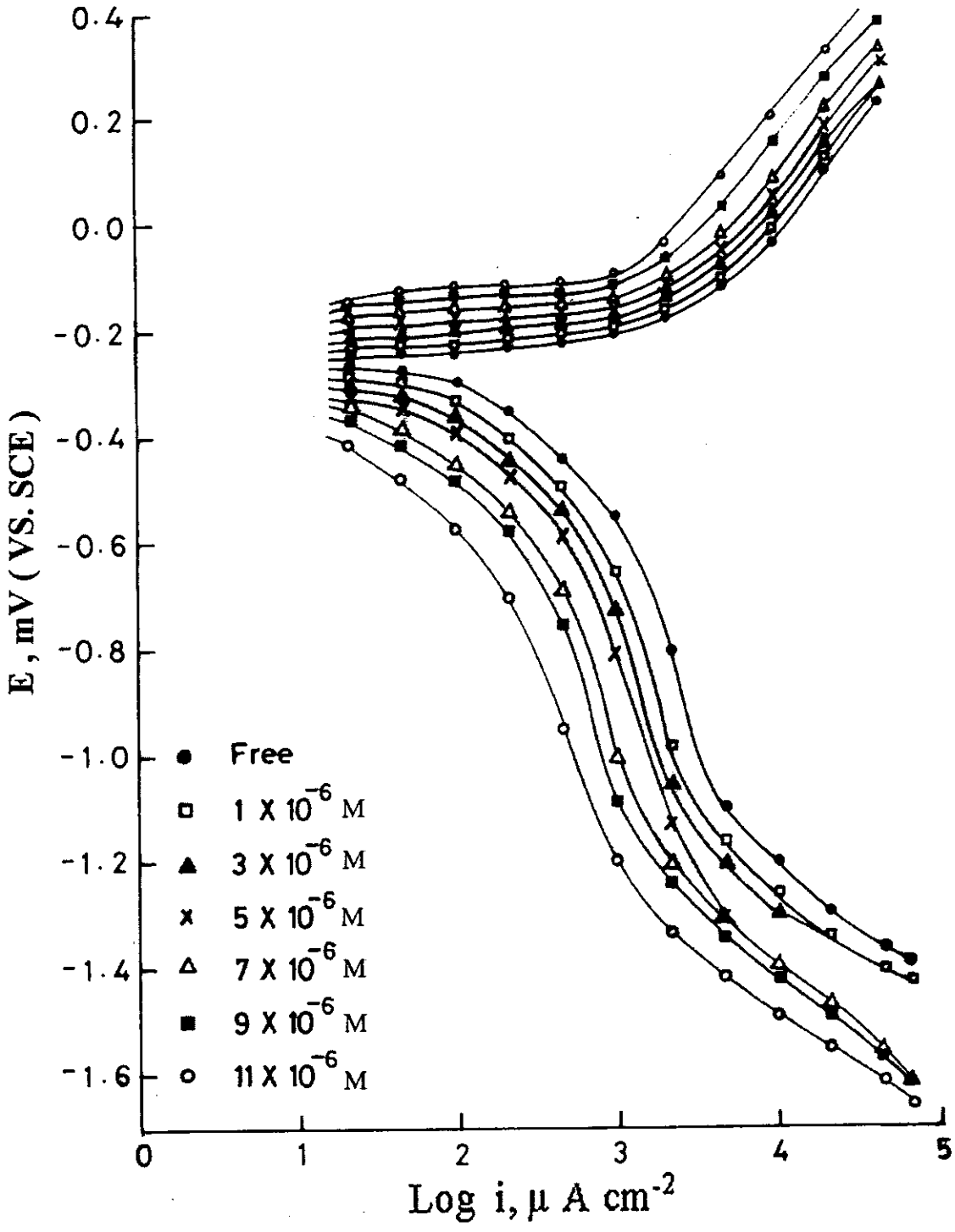

Fig.(3.34): Galvanostatic polarization curves of copper in 0.5 M HCl alone and containing different concentrations of compound (d).

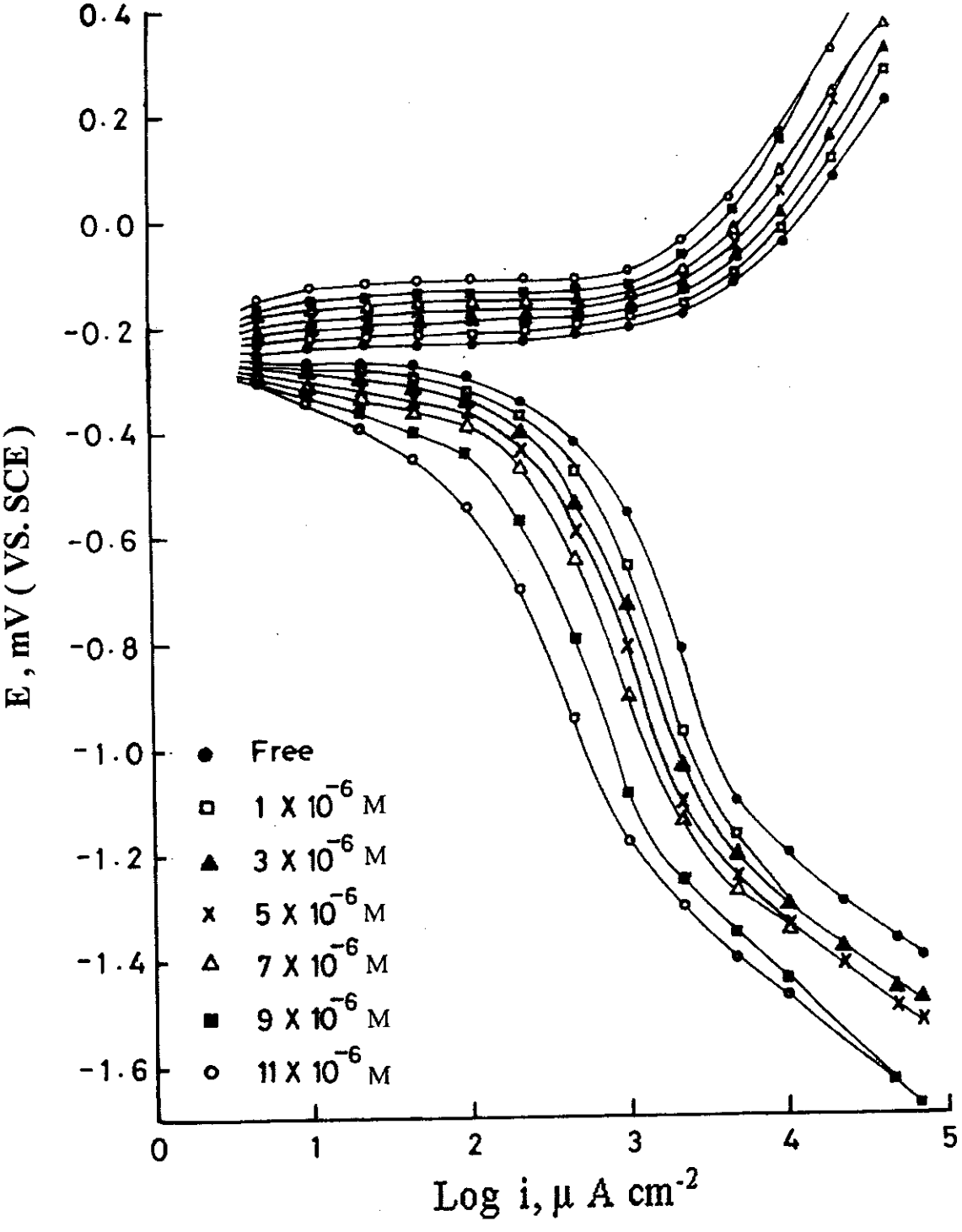

Fig.(3.35): Galvanostatic polarization curves of copper in 0.5 M HCl alone and containing different concentrations of compound (e).

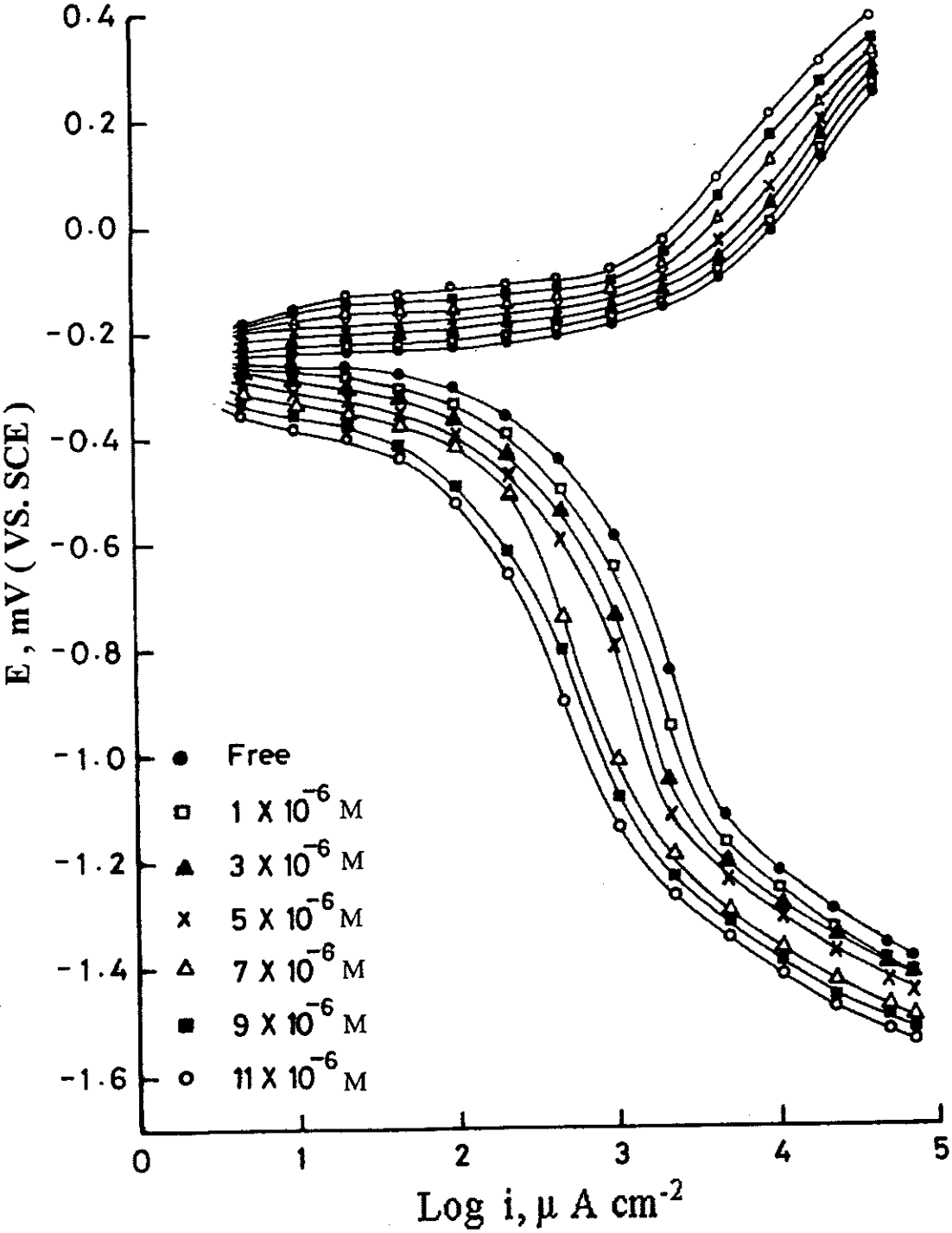

Fig.(3-36): Galvanostatic polarization curves of arsenic in 0·5 M HCl alone and containing different concentrations of compound (a).

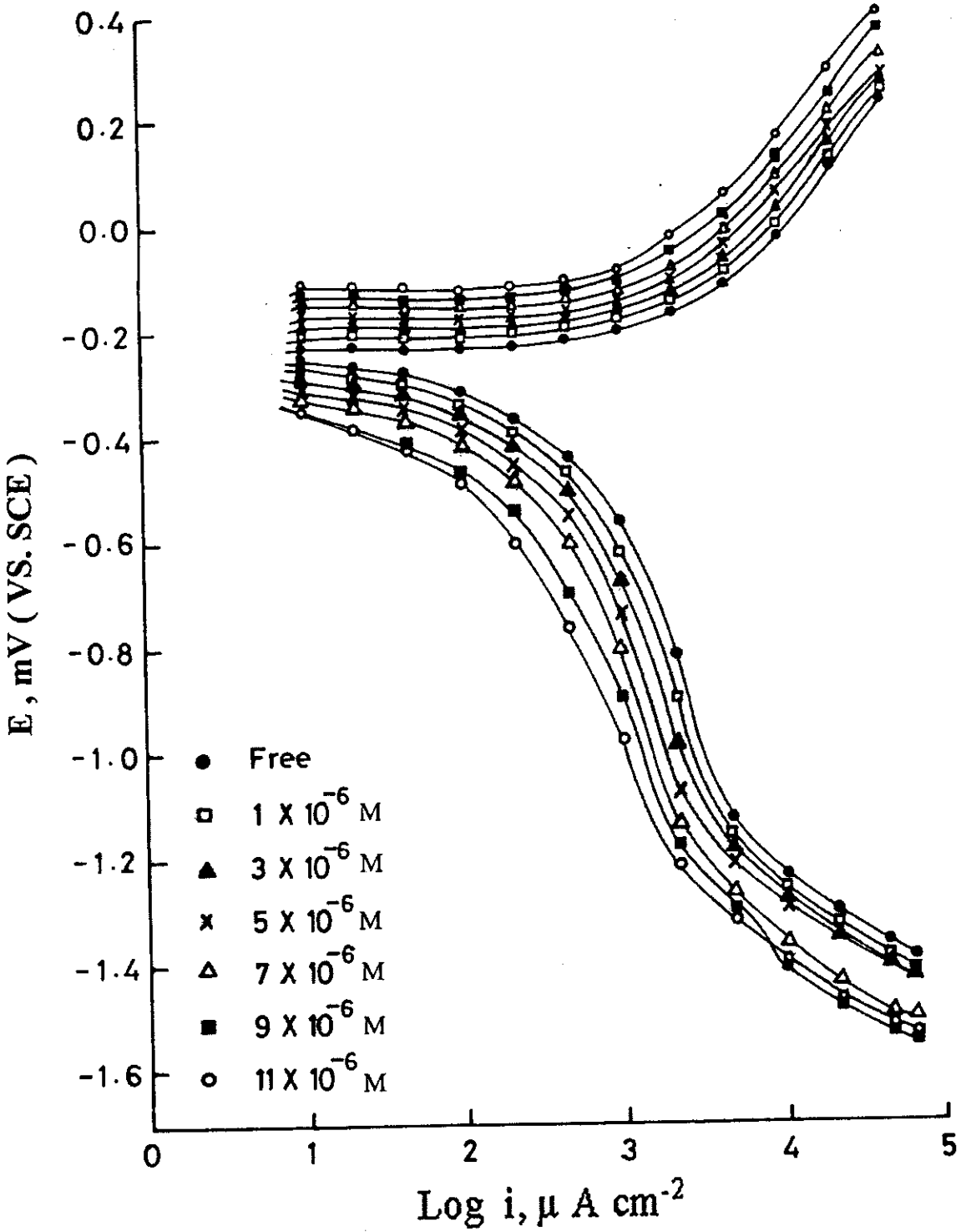

Fig.(3.37): Galvanostatic polarization curves of arsenic in 0.5 M HCl alone and containing different concentrations of compound (b).

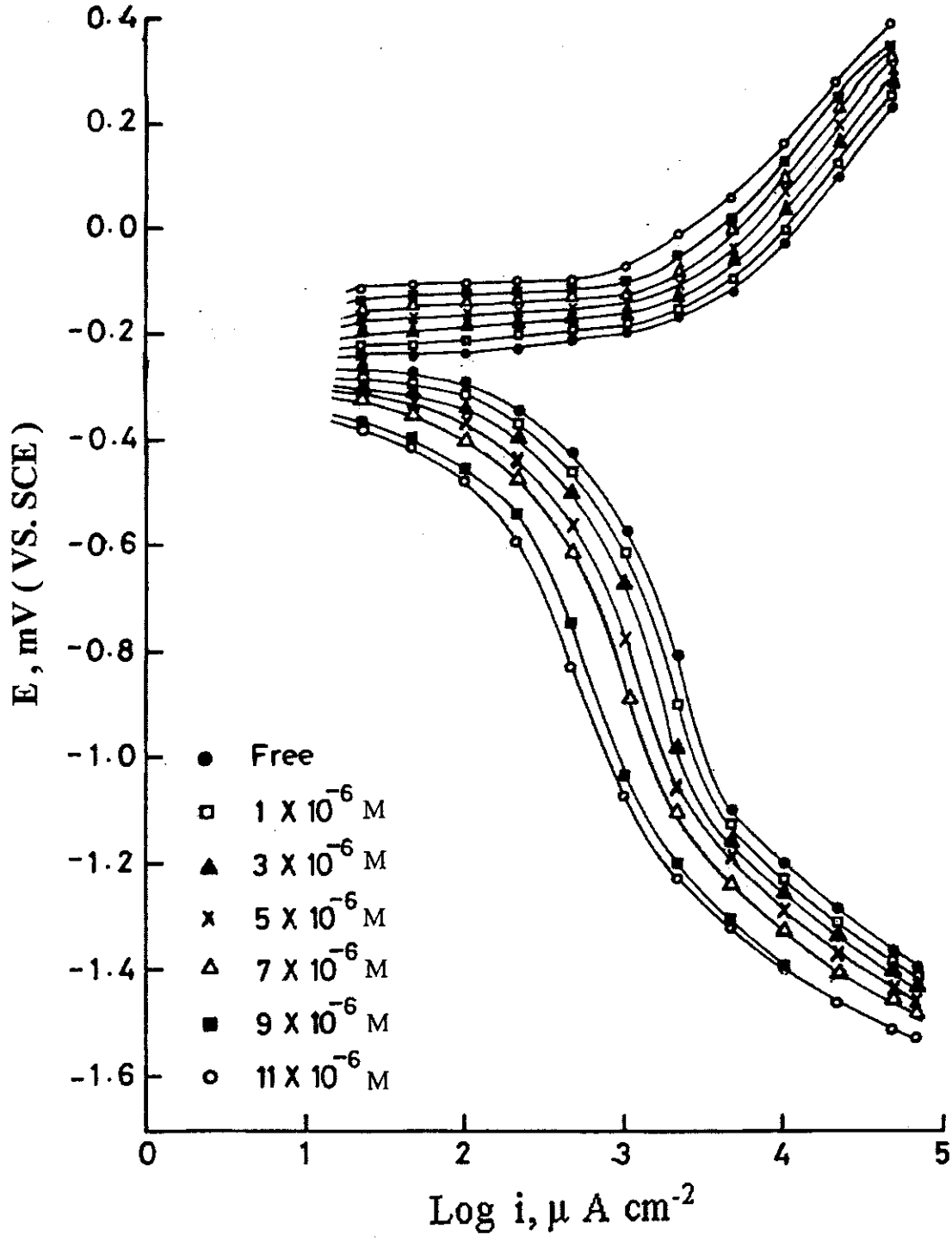

Fig.(3.38): Galvanostatic polarization curves of arsenic in 0.5 M HCl alone and containing different concentrations of compound (c).

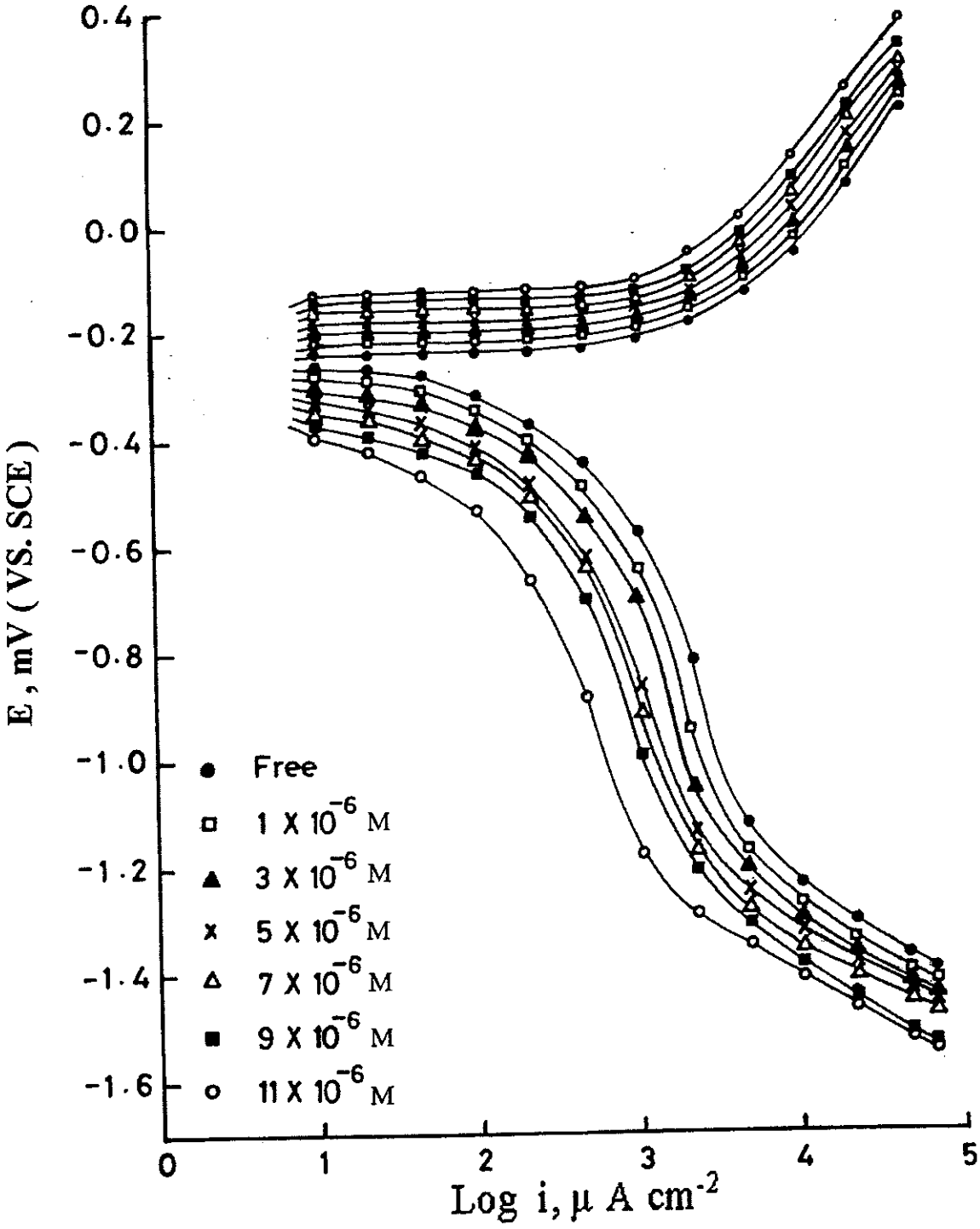

Fig.(3-39) : Galvanostatic polarization curves of arsenic in 0.5 M HCl alone and containing different concentrations of compound (d).

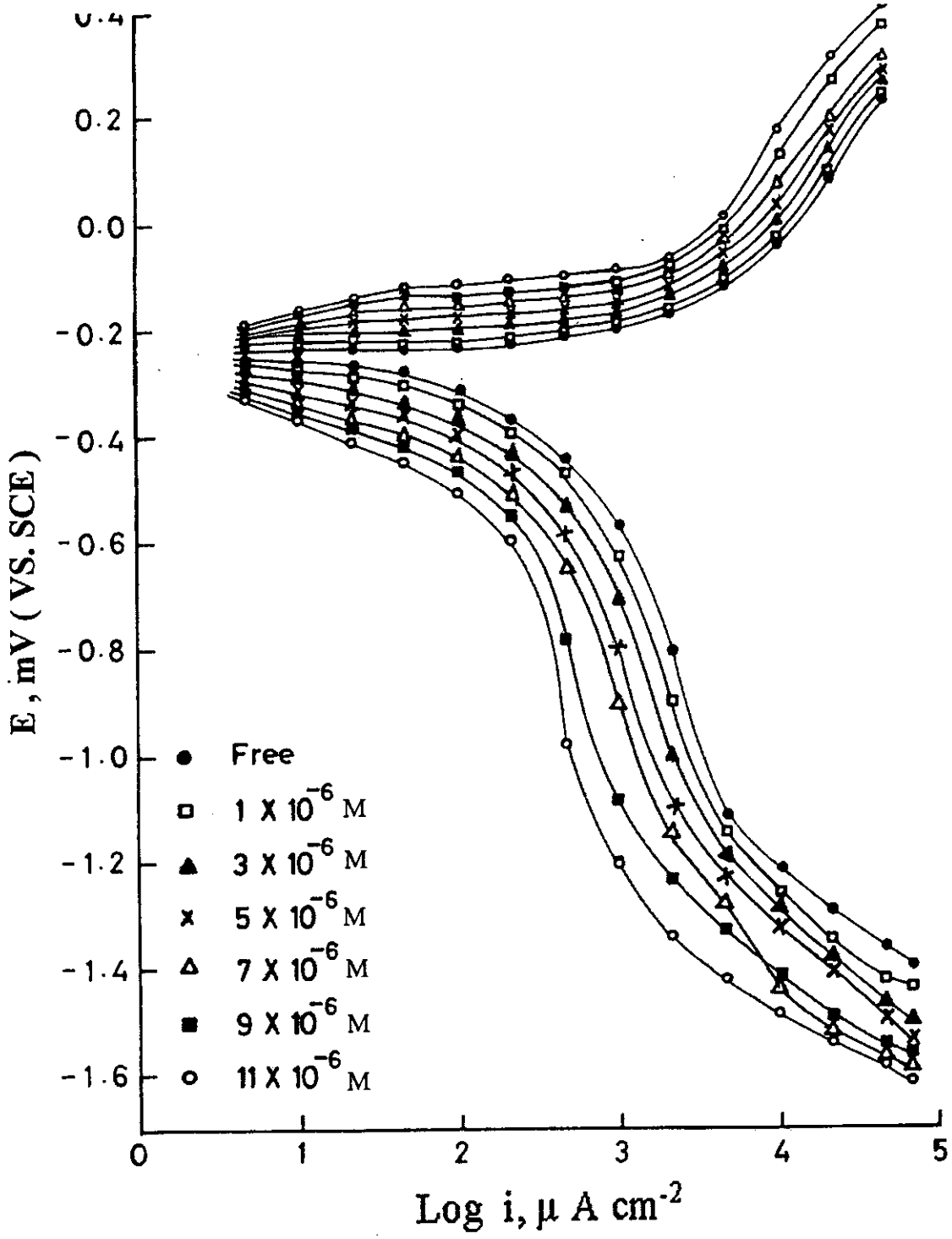

Fig.(3.40): Galvanostatic polarization curves of arsenic in 0.5 M HCl alone and containing different concentrations of compound (e).

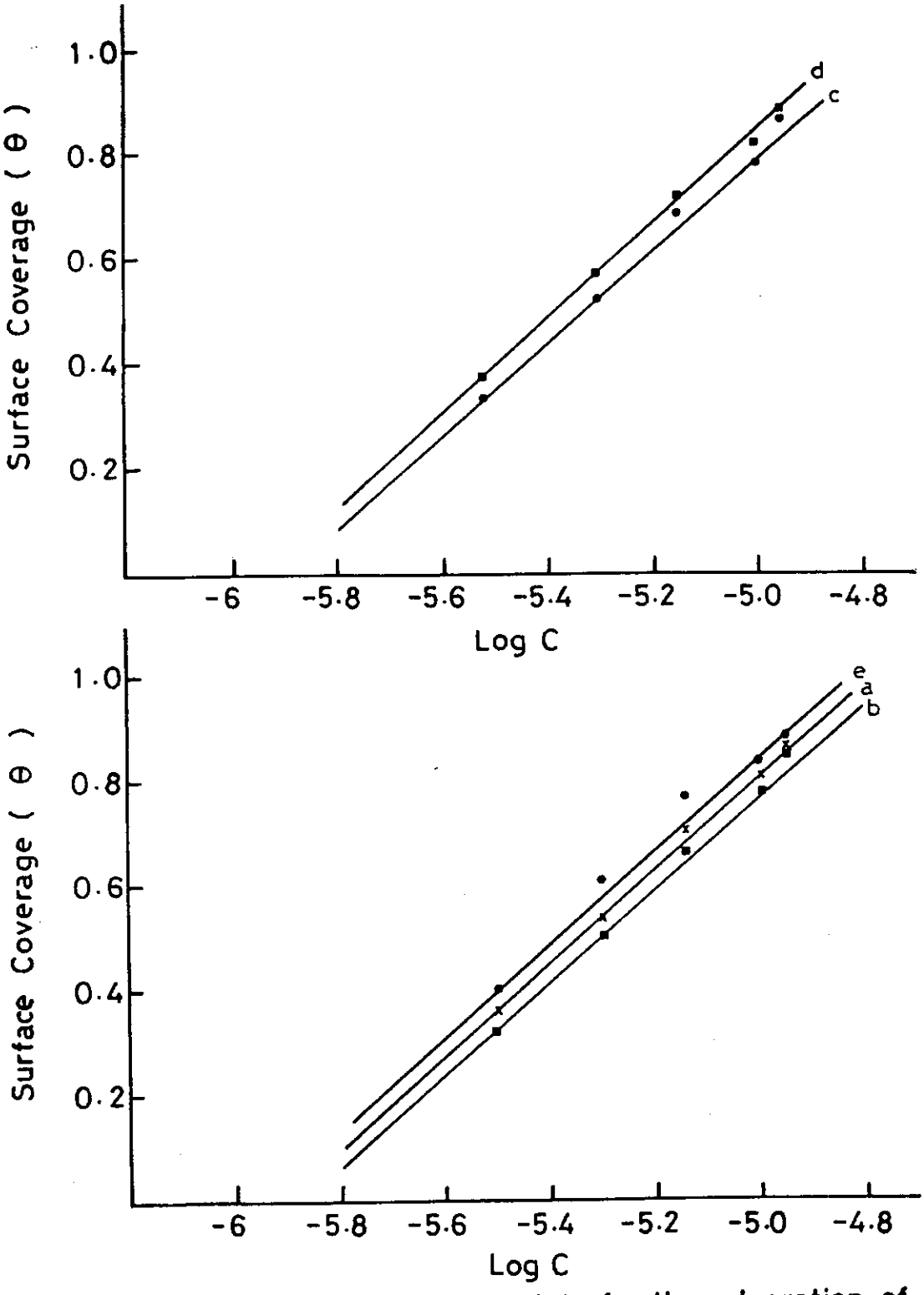

Fig(3.41) Temkin isotherm plots for the adsorption of benzylideneaniline derivatives on muntz in 0.5M HCl at 30°C.

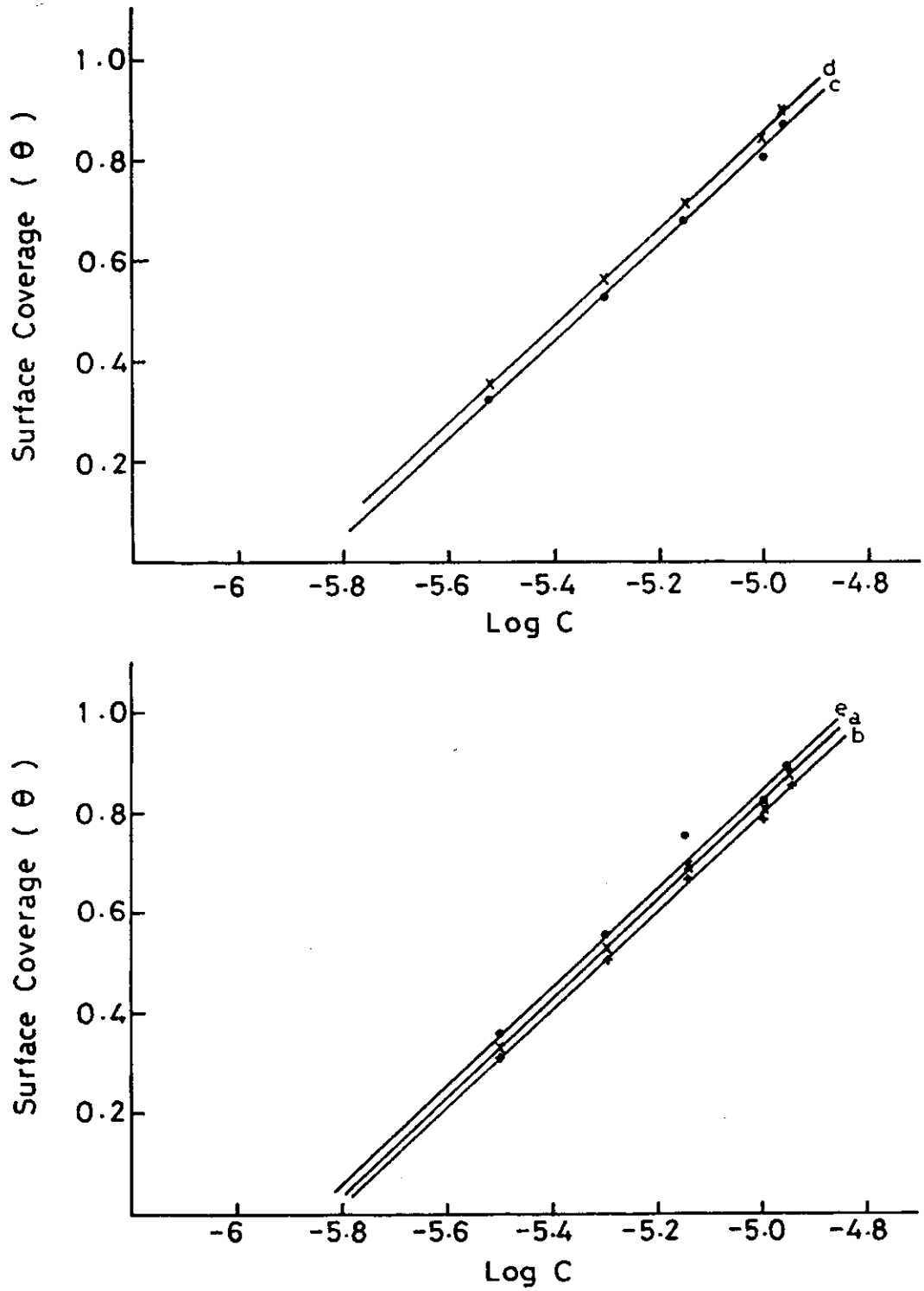

Fig(3.42) Temkin isotherm plots for the adsorption of benzylideneaniline derivatives on admiralty in 0.5 M HCl at 30 °C.

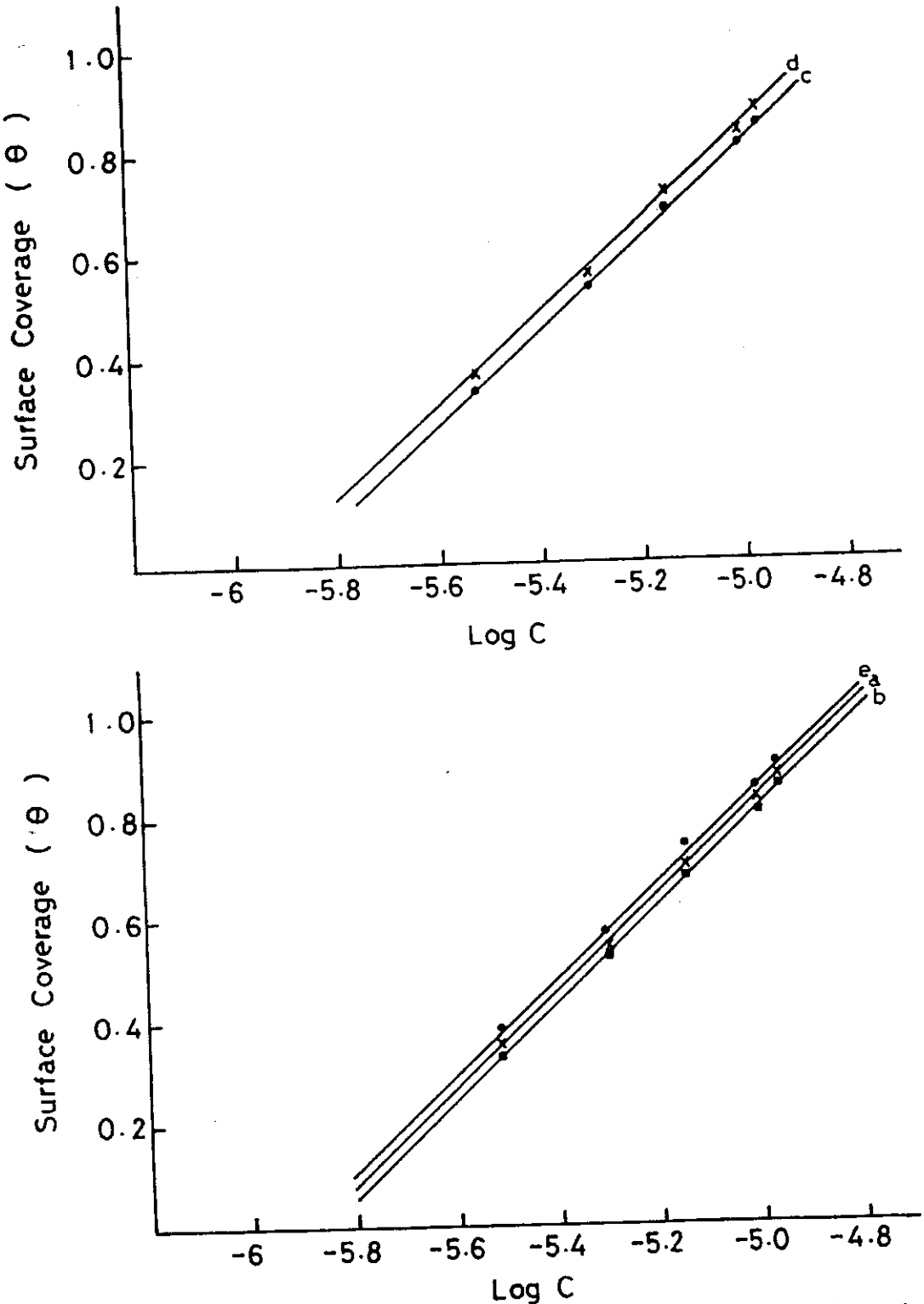

Fig(3.44)Temkin isotherm plots for the adsorption of benzylideneaniline derivatives on Arsenic in 0.5M HCl at 30 °C.

3.3- EFFECT OF TEMPERATURE

In this part the effect of temperature on the corrosion rate of copper and its alloys in 0.5M hydrochloric acid solution in absence and presence of $5x10^{-6}M$ of the benzylideneaniline derivatives was studied. The behaviour at different temperatures of range (30-60°C) was investigated by weight loss measurements. The values of corrosion rate obtained at different termperatures permit the calculation of the Arrhenius activation energy, E_a^*, according to the following equation

$$\log K = - E_a^* / 2.303RT + A \qquad (3.1)$$

where A is a constant depends on a metal type and the electrolyte. Arrhenius plot of logarithmic of corrosion rate (mg cm^{-2} min^{-1}) against the reciprocal of absolute temperature, 1/T, is shown graphically in Figures (3.45-3.48). The values of the activation energies, E_a^*, were calculated from the slopes of the straight lines. The values of the activation energies, E_a^*, for the dissolution of copper and its alloys in absence and presence of $5x10^{-6}M$ benzylideneaniline derivative compounds in 0.5M hydrochloric acid solution are given in Tables (3.30-3.33). These values indicate that the presence of benzylideneaniline derivatives increase the activation energy of the metal dissolution reaction and that the process is activation controlled. The activation energy, E_a^*, for the corrosion of copper and its alloys in 0.5M HCl [Figures (3.45-3.48)] is equal to 9.57-11.48. KJ/mol which is in good agreement with the work of Ammar et al. [159] which they found that the activation energy is 8.4 KJ/mol for copper in 0.1M HCl solution. On the other hand Gasparac et al. [160] found that the activation energy is 3.0 KJ/mol for copper in 0.5M HCl solution. On the other hand, Fouda et al.

[161] Mansour et al. [162] found that the activation energy of copper in 3M HNO_3 is equal to 30.6 KJ/mol and 72.4 KJ/mol, respectively. Generally one can say that the nature and concentration of electrolyte affect greatly the activation energy for the corrosion process. The addition of $5x10^{-6}$M of any one of the benzylideneaniline derivatives to the solution increase the activation energy (E_a^*), as shown in Tables (3.30-3.33) and the extent of the increase is proportional to the inhibition efficiency of the inhibitor, indicating that the energy barrier for the corrosion reaction increases in the presence of these additives. This means that by addition of the inhibitor in the acid solution, the corrosion reaction will be further pushed to surface sites that are characterized by higher values of, E_a^*. This indicates that copper corrosion occurs at the uncovered part of the surface. Thus, adsorption of the inhibitor was assumed to occur on the higher energy sites [163], the presence of inhibitor, which results in the blocking of the active sites, must be associated with an increase in the activation energy, E_a^*, of copper corrosion in the inhibited state.

Free energy of activation, ΔG^*, was calculated by applying the transition state equation

$$\Delta G^* = RT\left[\ln\frac{KT}{h} - \ln(\text{rate})\right] \qquad (3.2)$$

where, h = Plank's constant,

K = Boltzman's constant.

R = gas constant.

T = absolute temperature.

The enthalpy of activation ΔH^* and the entropy of activation ΔS^* were calculated by applying the following equations

$$\Delta H^* = E_a^* - RT \quad (3.3)$$

$$\Delta S^* = \frac{\Delta H^* - \Delta G^*}{T} \quad (3.4)$$

The values of the thermodynamic parameter for the dissolution of copper and its alloys, at different temperatures were calculated and given in Tables (3.30-3.33). Inspection of these data reveal that the values of ΔH^* and ΔG^* in the presence of the additives increase over that of the uninhibited solution. This implies that energy barrier of the corrosion reaction in the presence of benzylideneaniline derivatives increases, which is expected. ΔS^* in the absence and presence of a additives is larger and has negative values meaning that a decrease in disordering takes place in going from reactants to the activated complex [164,165]. From Tables (3.30-3.33) it is evident that the values of ΔG^* and ΔH^* increase with increasing temperature in absence and presence of $5x10^{-6}$M of the tested compounds.

Table (3-30). Thermodynamic activation parameters for muntz dissolution in 0.5M HCl in absence and presence of $5x10^{-6}$ M benzylideneaniline derivatives from weight loss measurement at different temperatures (E_a^* ,ΔH^*, ΔG^*: kcal.mol^{-1}, ΔS^* cal. mol^{-1} k^{-1}).

Temperature(K)	303	313	323	333
Free acid				
E_a^*	9.57			
ΔH^*	8.96	8.94	8.92	8.90
ΔG^*	10.14	10.16	10.19	10.22
$-\Delta S^*$	3.89	3.90	3.92	3.96
Inhibitor(*a*)				
E_a^*	15.31			
ΔH^*	14.7	14.68	14.65	14.61
ΔG^*	15.82	15.84	15.86	15.89
$-\Delta S^*$	3.70	3.72	3.75	3.84
Inhibitor(*b*)				
E_a^*	10.57			
ΔH^*	10.00	9.98	9.95	9.92
ΔG^*	11.69	11.83	11.92	11.98
$-\Delta S^*$	5.58	5.61	5.64	5.67
Inhibitor(*c*)				
E_a^*	11.48			
ΔH^*	10.9	10..87	10.84	10.80
ΔG^*	12.23	12.28	12.32	12.38
$-\Delta S^*$	4.38	4.41	4.43	4.46
Inhibitor(*d*)				
E_a^*	19.14			
ΔH^*	18.50	18.47	18.44	18.40
ΔG^*	19.28	19.32	19.36	19.39
$-\Delta S^*$	2.70	2.73	2.76	2.79
Inhibitor(*e*)				
E_a^*	22.97			
ΔH^*	21.90	21.88	21.85	21.83
ΔG^*	23.12	23.16	23.19	23.22
$-\Delta S^*$	4.03	4.07	4.10	4.15

Table(3-31). Thermodynamic activation parameters for admiralty dissolution in 0.5M HCl in absence and in presence of $5x10^{-6}$ M benzylideneaniline derivatives from weight loss measurement at different temperatures (E_a^* , ΔH^*, ΔG^* kcal.mol^{-1}, ΔS^* cal. mol^{-1} k^{-1}).

Temperature(K)	303	313	323	333
Free acid				
E_a^*	9.67			
ΔH^*	9.18	9.16	9.14	9.10
ΔG^*	11.13	11.16	11.17	11.21
$-\Delta S^*$	6.34	6.36	6.38	6.40
Inhibitor(*a*)				
E_a^*	15.36			
ΔH^*	14.66	14.64	14.62	14.60
ΔG^*	16.72	16.74	16.77	16.79
$-\Delta S^*$	6.66	6.71	6.74	6.78
Inhibitor(*b*)				
E_a^*	11.51			
ΔH^*	10.98	10.96	10.94	10.92
ΔG^*	12.28	12.31	12.35	12.39
$-\Delta S^*$	4.29	4.31	4.37	4.41
Inhibitor(*c*)				
E_a^*	13.31			
ΔH^*	12.68	12.66	12.64	12.62
ΔG^*	14.31	14.34	14.37	14.39
$-\Delta S^*$	5.38	5.40	5.43	5.46
Inhibitor(*d*)				
E_a^*	19.65			
ΔH^*	18.58	18.56	18.53	18.51
ΔG^*	20.22	20.24	20.26	20.28
$-\Delta S^*$	5.41	5.43	5.46	5.48
Inhibitor(*e*)				
E_a^*	23.23			
ΔH^*	22.66	22.63	22.60	22.57
ΔG^*	24.22	24.26	24.29	24.32
$-\Delta S^*$	5.15	5.21	5.24	5.26

Table(3-32). Thermodynamic activation parameters for copper dissolution in 0.5M HCl in absence and in presence of $5x10^{-6}$ M benzylideneaniline derivatives from weight loss measurement at different temperatures(E_a^* ,ΔH^*, ΔG^*: kcal.mol^{-1}, ΔS^* cal. mol^{-1} k^{-1}).

Temperature(K)	303	313	323	333
Free acid				
E_a^*	9.87			
ΔH^*	9.28	9.26	9.24	9.21
ΔG^*	11.30	11.33	11.36	11.39
$-\Delta S^*$	6.67	6.69	6.72	6.75
Inhibitor(*a*)				
E_a^*	17.22			
ΔH^*	16.66	16.64	16.61	16.58
ΔG^*	18.70	18.72	18.75	18.79
$-\Delta S^*$	6.61	6.65	6.68	6.70
Inhibitor(*b*)				
E_a^*	12.48			
ΔH^*	11.89	11.86	11.84	11.81
ΔG^*	13.81	13.84	13.86	13.89
$-\Delta S^*$	6.34	6.32	6.25	6.22
Inhibitor(*c*)				
E_a^*	15.22			
ΔH^*	14.64	14.62	14.59	14.57
ΔG^*	16.42	16.44	16.47	16.49
$-\Delta S^*$	5.87	5.81	5.79	5.75
Inhibitor(*d*)				
E_a^*	20.14			
ΔH^*	19.58	19.56	19.52	19.49
ΔG^*	21.41	21.43	21.46	21.49
$-\Delta S^*$	6.04	5.98	5.96	5.93
Inhibitor(*e*)				
E_a^*	22.64			
ΔH^*	21.98	21.96	21.94	21.91
ΔG^*	23.82	23.84	23.87	23.89
$-\Delta S^*$	6.07	6.01	5.98	5.95

Table(3-33). Thermodynamic activation parameters for arsenic dissolution in 0.5M HCl in absence and in presence of $5x10^{-6}$ M benzylideneaniline derivatives from weight loss measurement at different temperatures (E_a^*,ΔH^*, ΔG^*: kcal.mol^{-1}, ΔS^* cal. mol^{-1} k^{-1}).

Temperature(K)	303	313	323	333
Free acid				
E_a^*	11.48			
ΔH^*	10.88	10.86	10.84	10.82
ΔG^*	12.72	12.74	12.76	12.78
$-\Delta S^*$	6.07	6.01	5.94	5.88
Inhibitor(*a*)				
E_a^*	16.35			
ΔH^*	15.80	15.78	15.76	15.73
ΔG^*	17.54	17.56	17.58	17.61
$-\Delta S^*$	5.74	5.69	5.63	5.61
Inhibitor(*b*)				
E_a^*	13.48			
ΔH^*	12.76	12.74	12.72	12.71
ΔG^*	14.66	14.68	14.70	14.73
$-\Delta S^*$	6.27	6.20	6.13	6.07
Inhibitor(*c*)				
E_a^*	15.43			
ΔH^*	14.82	14.80	14.77	14.75
ΔG^*	16.63	16.66	16.68	16.71
$-\Delta S^*$	5.97	5.94	5.91	5.88
Inhibitor(*d*)				
E_a^*	21.05			
ΔH^*	20.52	20.50	20.47	20.45
ΔG^*	22.28	22.30	22.32	22.35
$-\Delta S^*$	5.81	5.75	5.73	5.71
Inhibitor(*e*)				
E_a^*	23.85			
ΔH^*	22.98	22.96	22.94	22.90
ΔG^*	25.06	25.08	25.11	25.13
$-\Delta S^*$	6.86	6.77	6.72	6.65

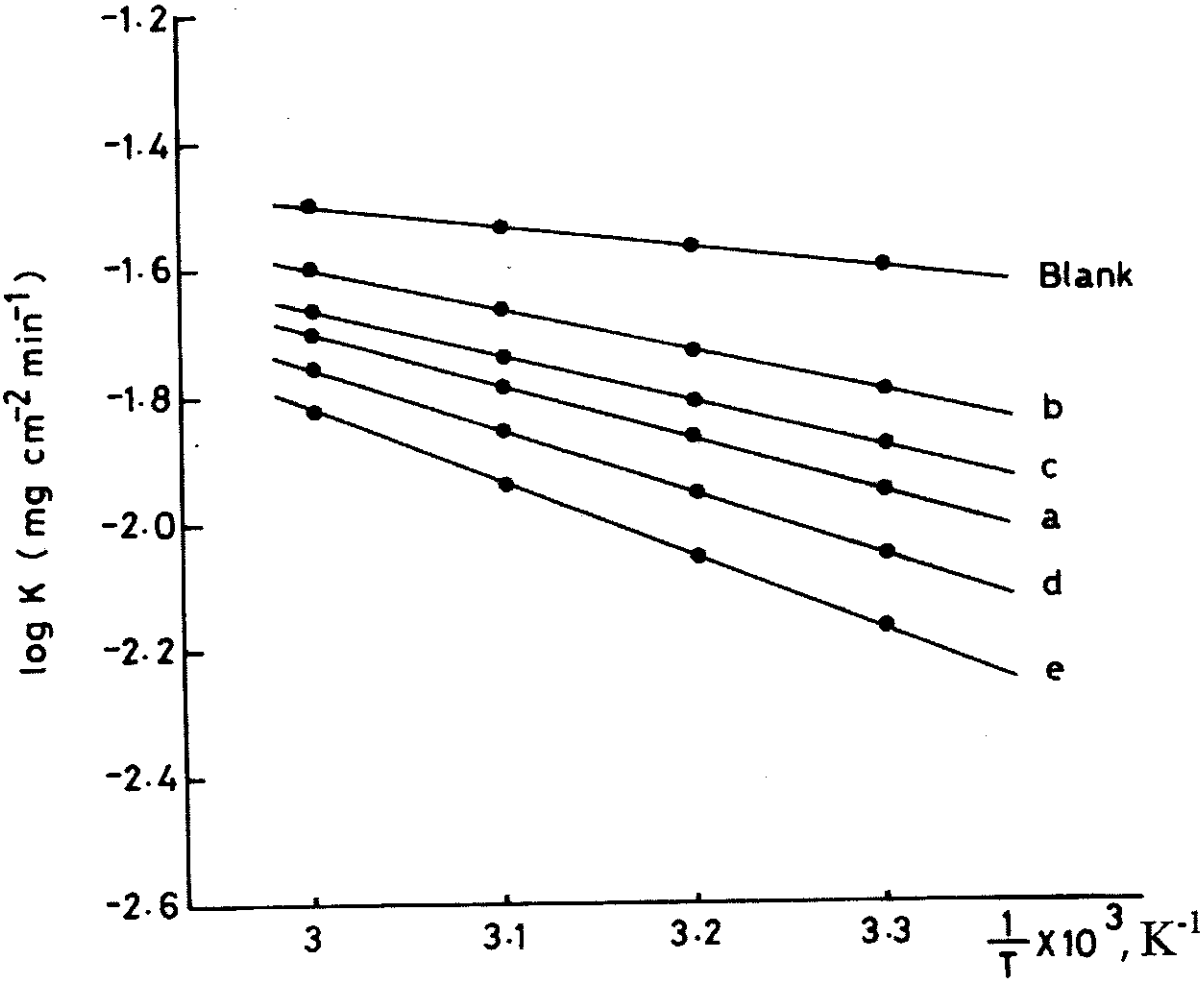

Fig. (3.45): log K - $\frac{1}{T}$ Curves For Muntz in presence and absence of different inhibitors.

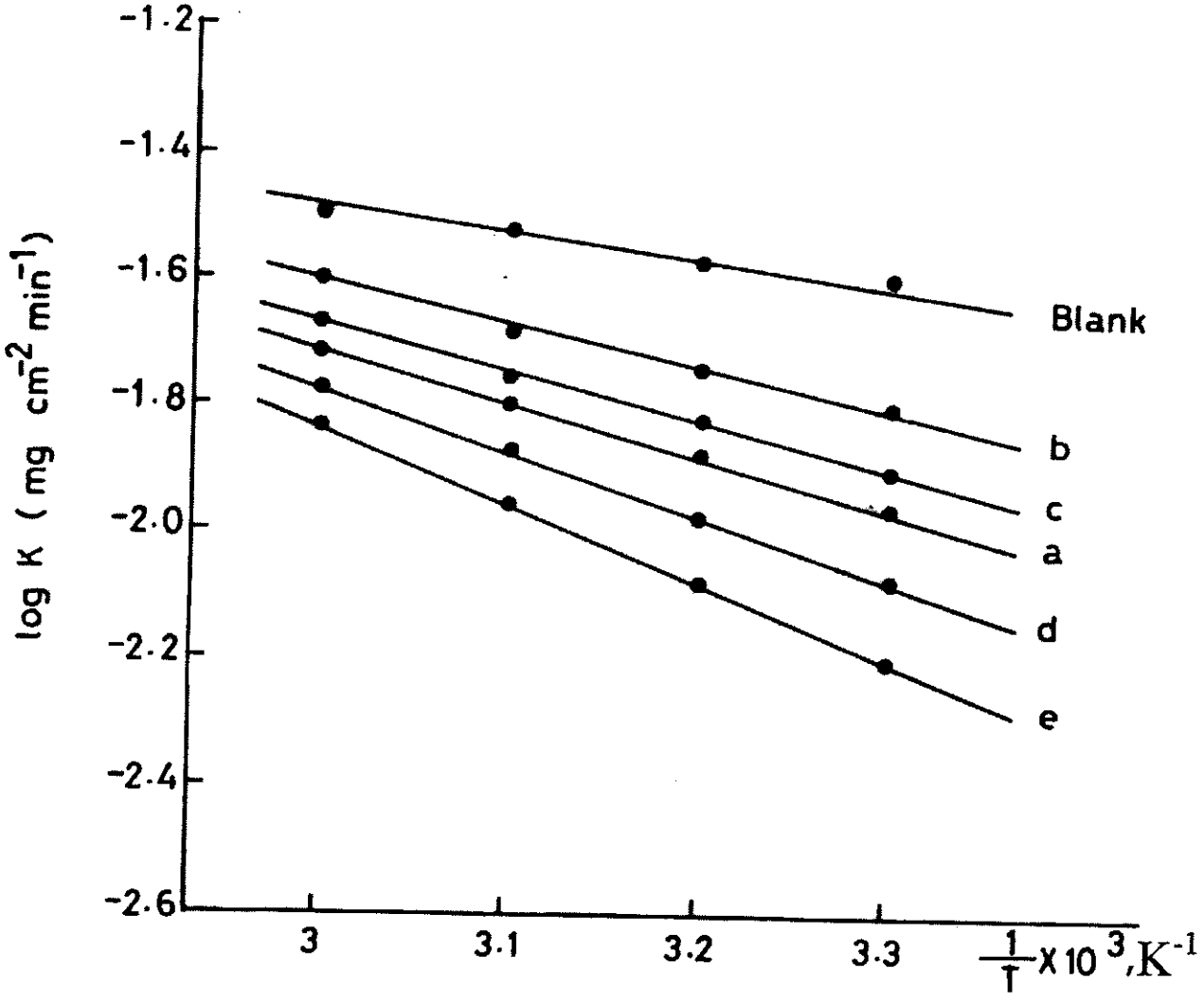

Fig.(3.46): log K-$\frac{1}{T}$ Curves For Admiralty in presence and absence of different inhibitors.

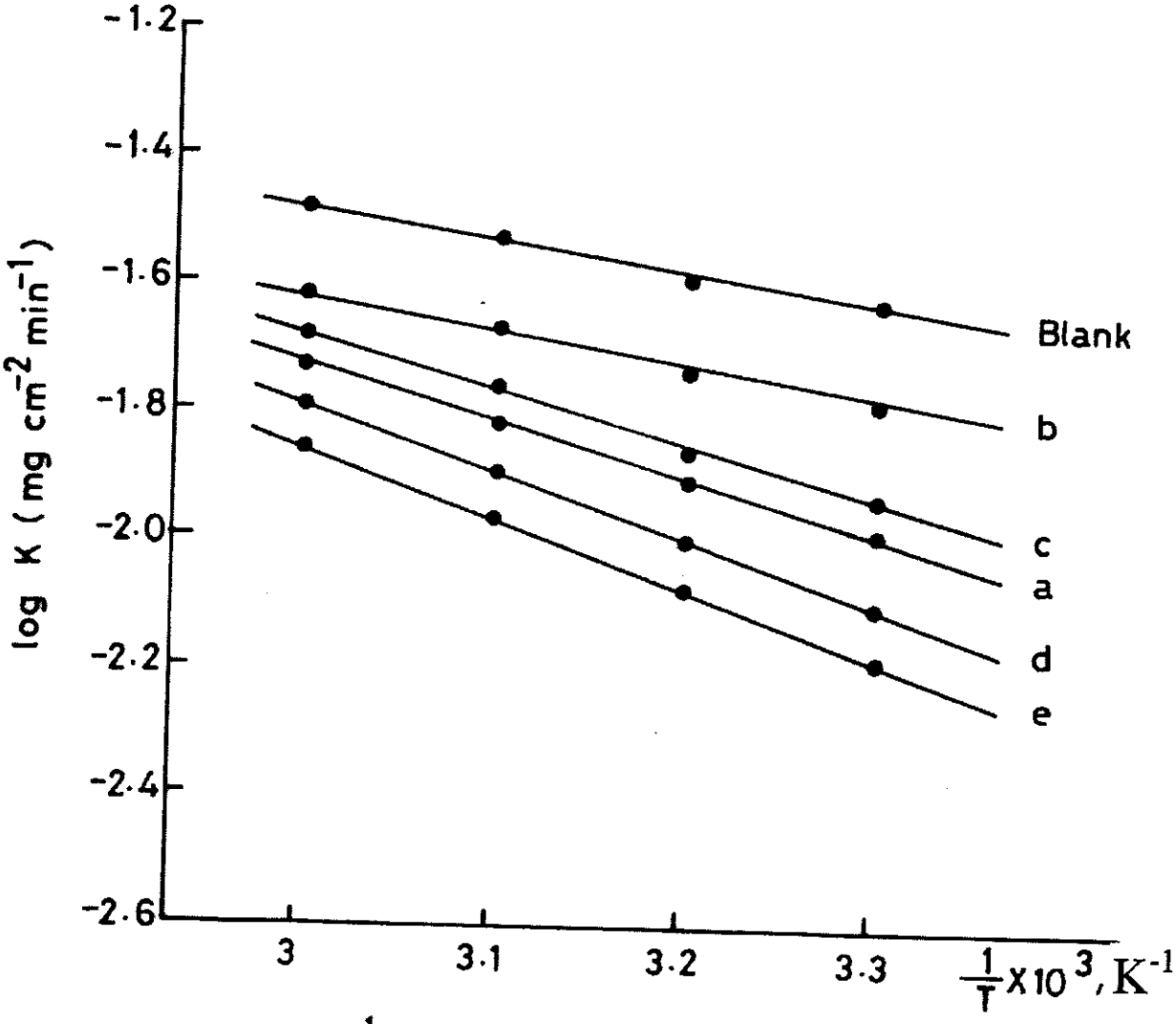

Fig.(3.47): log K - $\frac{1}{T}$ Curves For Copper in presence and absence of different inhibitors.

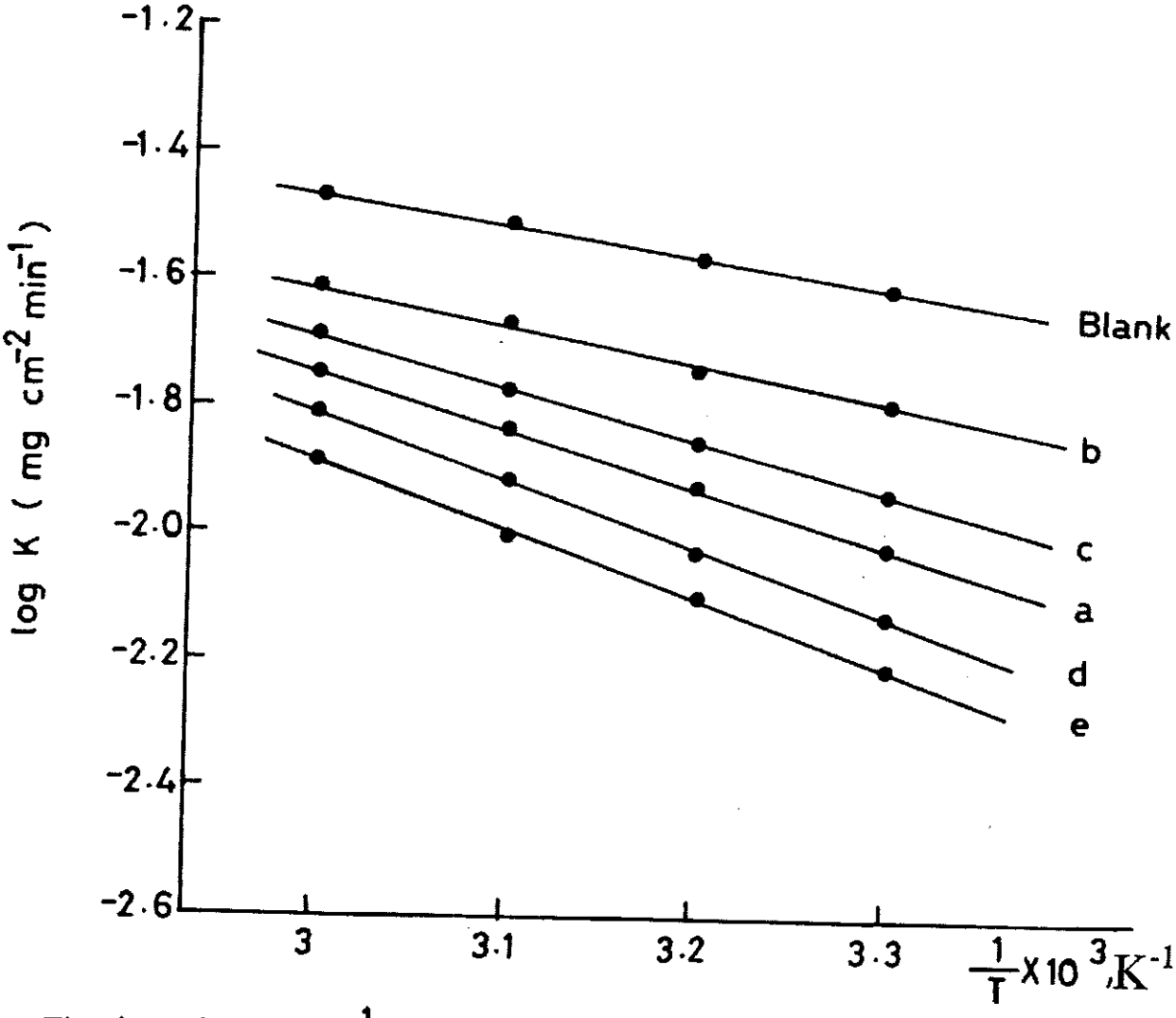

Fig.(3.48): log K-$\frac{1}{T}$ Curves For Arsenic in presence and absence of different inhibitors.